Centre for
**Process
Systems
Engineering**

Professor Efstratios Pistikopoulos
Centre for Process Systems Engineering
Imperial College London

AVT **AACHENER
VERFAHRENS-
TECHNIK**

Professor Wolfgang Marquardt
Institute for Process Systems Engineering
RWTH Aachen University

PSE

Professor Constantinos Pantelides
Process Systems Enterprise
Managing Director

Capital Cost Evaluation for Optimum Process Design of Cryogenic Air Separation

Diploma Thesis
by
Robert Pack

London, SS 2012

Diploma Thesis
for
Mr. Robert Pack

Task Description

Current air separation process optimization is carried out sequentially with various discrete or continuous process parameters, and then iterated with equipment sizing and costing. Typical process parameters include temperature, pressure, flow, pressure drop, product purity, distillation column feed and/or draw locations staging, and etc. Major equipment used in cryogenic air separation include air compressors, turbines, plate and fin heat exchangers, cooler, distillation columns, condensers, reboilers, and etc. Once process optimum condition is identified, individual equipment is sized and cost estimated. Capital cost is then feed back to process to verify the original optimum condition. If the original optimum condition changes, we will have to re-optimize the process parameter and identify the new process optimum condition. New equipment sizing and costing will have to be adjusted accordingly.

The deficiency of the current process is apparent: manual, sequential and iterative. We would like to streamline the optimization process, incorporate the capital equipment cost into the process optimization. The process optimizer we target is gPROMS. The goal is to simultaneously optimize process and equipment to minimize the total process cost with user defined objective functions.

Prof. Efstratios Pistikopoulos

Prof. Dr.-Ing. Wolfgang Marquardt

Betreuer der Arbeit: Dipl. Ing. Mirko Skiborowski
Tag der Abgabe: xx.xx.2012

Statutory Declaration

I herewith declare that I have completed the present thesis independently making use only of the specified literature and aids. Sentences or parts of sentences quoted literally are marked as quotations; identification of other references with regard to the statement and scope of the work is quoted. The thesis in this form or in any other form has not been submitted to an examination body and has not been published.

_____

Date   Signature

Contents

Contents

List of Figures

List of Tables

Nomenclature

POT	Payout time	[$]
a	Annuity	[$]
C_0	Initial value of an investment	[$]
C_n	Final value of an investment	[$]
C_{0e}	Present value of all expenses	[$]
C_{0r}	Present value of all revenues	[$]
i	Interest rate	[%]
NPV	Net present value	[$]
q	Interest factor	[−]
$\dot{e}_{ij}$	Energy flow of to equipment i from energy carrier j	[kW]
$\dot{m}_i$	Mass flow of component i	[$\frac{kg}{s}$]
C_B^i	Reference cost of equipment i	[$]
C_E^i	Cost of equipment i	[$]
C_{EC}^i	Mass specific cost of energy carrier i	[$\frac{\$}{kW}$]
C_{RM}^i	Mass specific cost of raw material i	[$\frac{\$}{kg}$]
C_1	Reference equipment cost at time 1	[$]
C_2	Reference equipment cost at time 2	[$]
C_P	Total process cost	[$]
C_P^0	Reference process cost	[$]
C_{EC}	Total cost of energy	[$]

C_{FILL}	Cost of raw materials to fill the process	[$]
C_{RM}	Total cost of raw materials	[$]
f_C^i	Design complexity correction to equipment cost	[−]
f_M^i	Material selection correction to equipment cost	[−]
f_P^i	Pressure correction to equipment cost	[−]
f_T^i	Temperature correction to equipment cost	[−]
I_1	Cost index at time 1	[−]
I_2	Cost index at time 2	[−]
M^i	Equipment specific factor	[−]
N_E	Number of equipment pieces in the process	[−]
N_{RM}	Number of raw materials	[−]
Q^i	Specific quantity for equipment i	[$variable$]
Q_B^i	Equipment specific reference quantity	[$variable$]
Q_P	Process capacity	[$\frac{kg}{h}$]
Q_P^0	Reference process capacity	[$\frac{kg}{h}$]
t_{op}	Time of process operations	[s]
x	Degression coefficient	[−]

Greek Letters

γ_i	liquid activity coefficient of component i	[−]
μ_S	isentropic expansion coefficient	[$\frac{K}{Pa}$]
μ_{JT}	*Joule-Thompson* coeffivcient	[$\frac{K}{Pa}$]
ν^D	reflux ratio	[−]
ν^R	boliup ratio	[−]
ν^{vap}	condenser vapour fraction	[−]

φ_i^0	reference vapour fugacity coefficient of component i	$[-]$
φ_i	vapour fugacity coefficient of component i	$[-]$
ζ_{ij}^L	splitting variable for liquid feed i on stage j	$[-]$
ζ_j^R	splitting variable for reboiler reflux on stage j	$[-]$
ζ_{ij}^{SL}	splitting variable for liquid side draw i on stage j	$[-]$
ζ_{ij}^{SV}	splitting variable for vapour side draw i on stage j	$[-]$
ζ_{ij}^V	splitting variable for vapour feed i on stage j	$[-]$

Variables

Δp	pressure drop over entire column	$[Pa]$
Δp_{stage}	stage-wise pressure drop	$[Pa]$
a_c	parameter in Peng-Robinson EOS	$[\frac{m^5}{mol^2 s^2}]$
b	parameter in Peng-Robinson EOS	$[\frac{m^3}{mol}]$
C	number of components	$[-]$
F_j^L	molar liquid feed flowrate to stage j	$[\frac{mol}{s}]$
F_j^V	molar vapour feed flowrate to stage j	$[\frac{mol}{s}]$
f_i^L	liquid fugacity	$[-]$
f_i^V	vapour fugacity	$[-]$
F_j^L	Liquid feed to tray j	$[\frac{mol}{s}]$
F_j^V	Vapour feed to tray j	$[\frac{mol}{s}]$
F_{Pi}	compressibility factor of component i	$[-]$
h_j^L	molar liquid enthalpy on stage j	$[\frac{J}{mol}]$
h_j^V	molar vapour enthalpy on stage j	$[\frac{J}{mol}]$
h_j^{FL}	molar liquid feed enthalpy to stage j	$[\frac{J}{mol}]$
h_j^{FV}	molar vapour feed enthalpy to stage j	$[\frac{J}{mol}]$

K_{ij}	equilibrium ratio of component i on stage j	$[-]$
L_j	Liquid flow from tray j	$[\frac{mol}{s}]$
L_j	molar liquid flowrate form stage j	$[\frac{mol}{s}]$
l_{ij}	liquid molar flowrate of component i from stage j	$[\frac{mol}{s}]$
m	parameter in Peng-Robinson EOS	$[-]$
N	number of stages	$[-]$
p	pressure	$[Pa]$
p	system pressure	$[Pa]$
p_i^S	vapour pressure of component i	$[Pa]$
S_j^L	molar liquid side-draw flowrate form stage j	$[\frac{mol}{s}]$
S_j^V	molar vapour side-draw flowrate form stage j	$[\frac{mol}{s}]$
s_j^V	dimensionless liquid side-draw from stage j	$[-]$
s_j^V	dimensionless vapour side-draw from stage j	$[-]$
S_j^L	Liquid side flow from tray j	$[\frac{mol}{s}]$
S_j^V	Vapour side flow from tray j	$[\frac{mol}{s}]$
T^{bub}	bubble point temperature	$[K]$
T^{dew}	dew point temperature	$[K]$
V_j	Vapour flow from tray j	$[\frac{mol}{s}]$
V_j	molar vapour flowrate form stage j	$[\frac{mol}{s}]$
v_{ij}	vapour molar flowrate of component i from stage j	$[\frac{mol}{s}]$
x_{ij}	liquid mole fraction of component i on stage j	$[-]$
y_{ij}	vapour mole fraction of component i on stage j	$[-]$
z_{ij}^L	liquid mole fraction of liquid feed to stage j	$[-]$
z_{ij}^V	vapour mole fraction of vapour feed to stage j	$[-]$

Abstract

here comes an abstract

1 Introduction

Air separation technology, or – more generally speaking – gas separation technology, lies at the heart of the modern process industry. Highly pure oxygen and nitrogen ore uses in many industrial applications. Modern power generation processes, such as the currently developed OXICOAL process, rely on incineration with pure oxygen to produce flue gases with very high carbon dioxide content for further storage. Nitrogen is essential to many widely used processes such as the production of ammonia in the Haber-Bosch synthesis, as fertilizer or in many organic reactions.

The papaer followin this introduction is structured as follws....

Figure 1.1: Demand for industrial gases. []
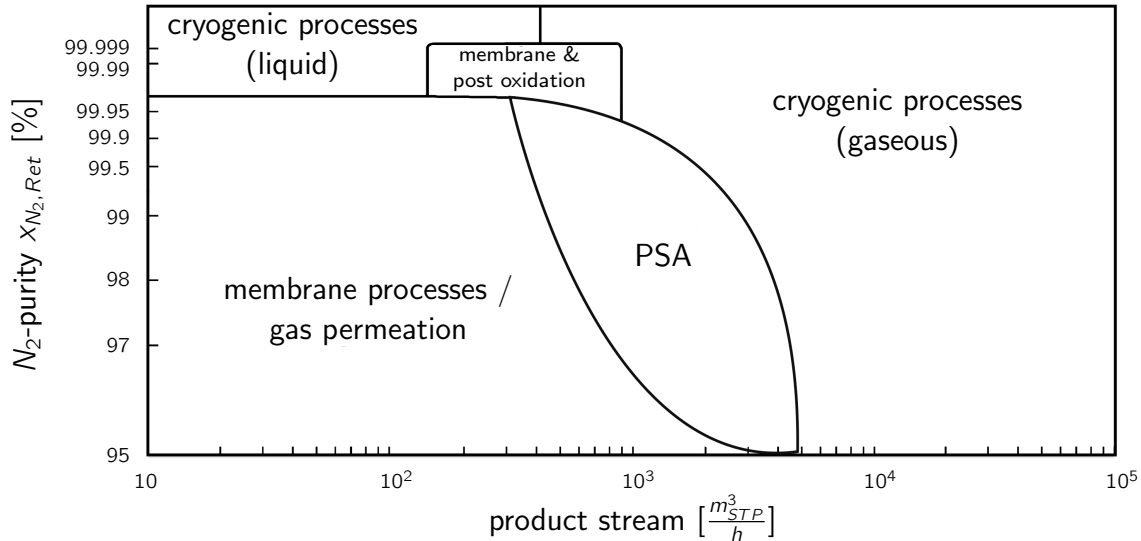
2 Air separation technology

Figure 2.1: Comparison of Air Separation Technologies [21].

There are several ways besides cryogenic air separation that can be employed to separate gas mixtures. In this chapter different competing technologies and their main applications will be discussed. The predominately used technologies are cryogenic distillation, pressure swing adsorption (PSA) as well as gas permeation (GP). In the distillation process the gas is first liquefied. Separation is the achieved by the different concentration differences in vapor and liquid phase. PSA relies on the different affinities of gaseous species to adsorb to certain materials in order to extract a component form a mixture. During gas permeation membranes are used. Each species migrates in different quantities through a given membrane depending on process parameters and membrane structure.

fig. 2.1 illustrates the most economically viable processes depending on product purity and product stream volume. It can be seen that alternative air separation processes cannot supply the high quality or quantity of the cryogenic process. Due to that cryogenic air separation is thought to be the main supplier of highly pure gases in industrial quantities for years to come [9]. The alternative processes however offer some very appealing characteristics, which make them the favorable choice when lower quantities of product or more moderate purity is required. The cryogenic process is always connected with an considerable energy consumption for the liquefaction and compression. Due to that smaller implementations of the process a very unlikely to yield economically sound solutions to a separation problem.
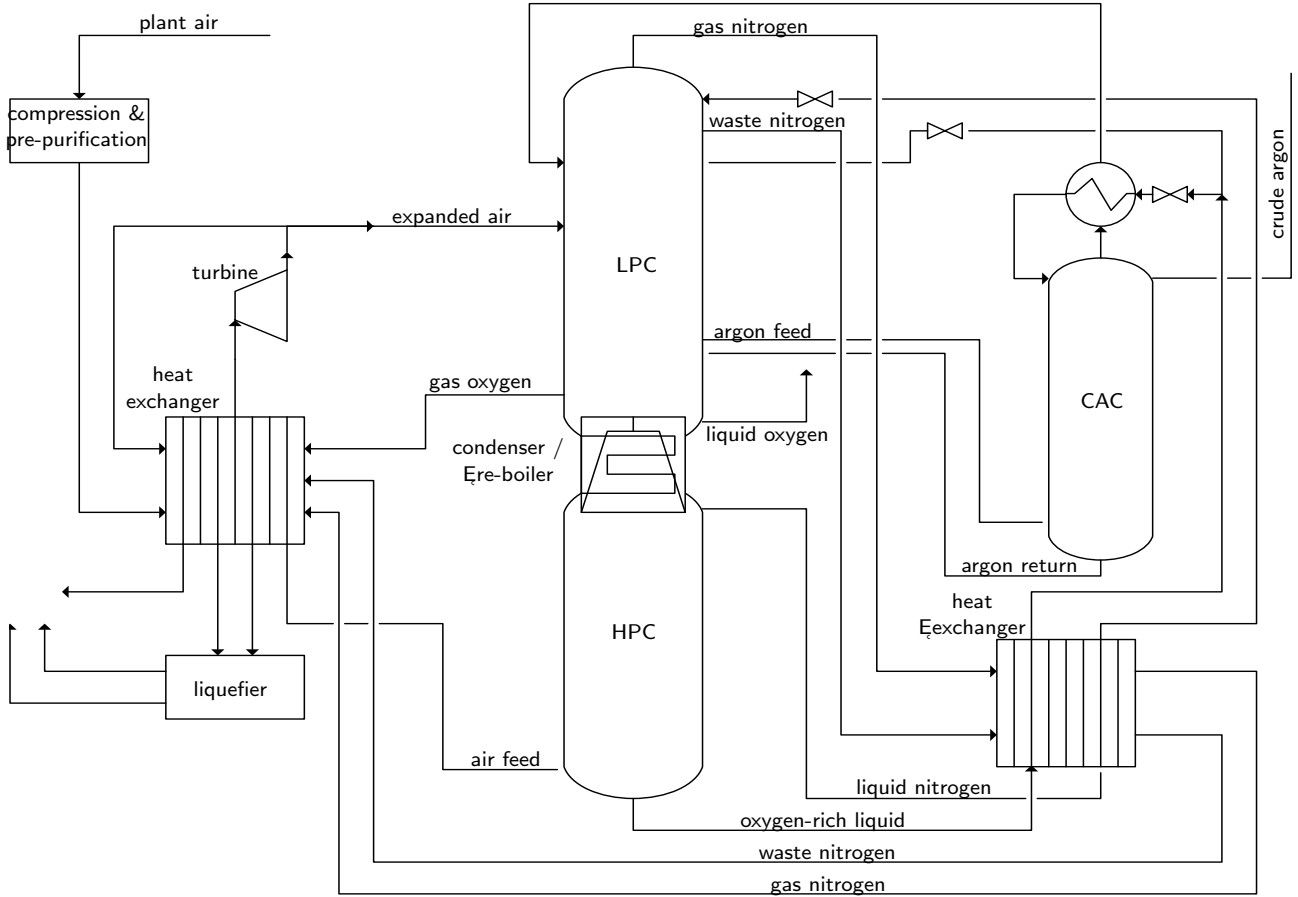
Figure 2.2: Schematic representation of the cryogenic air separation process.

2.1 Cryogenic air separation

Cryogenic Air Separation finds applications over a great variety of industries among others refining, petrochemicals, medical, food & beverages and environmental [23]. Furthermore prospective processes for power generation from fossil sources in form of the integrated gaseous combined cycle (IGCC) integrates the air separation process in order to enable more environmentally friendly power generation [18].

As can be seen in fig. 2.2 double effect heat integrated distillation column lies at the heart of the air liquefaction processes. It consists of a high pressure column (HPC) operating at 0.68 MPa and temperatures below 130 K as well as a low pressure column (LPC) which operates at around 0.13 MPa an comparable temperatures. In order to also attain highly pure argon as a product the process may also include a crude argon column (CAC) which works at slightly lower pressures than the LPC.

The plant air entering the process is initially purified, where carbon and nitrogen oxides as well as solid contaminants are removed, and then compressed to process conditions. The compressed air is then cooled against product streams namely liquefied nitrogen, oxygen and argon. The air stream is then divided into several sub-streams. One of those is fed into the HPC bottom, while another is expanded by means of a turbine and further cooled down through the Joule- Thompson effect. Aside from further cooling energy from the initial compression is thus partially recovered. This expanded air stream is then fed into the LPC. At the bottom of the LPC liquid as well as gaseous oxygen are
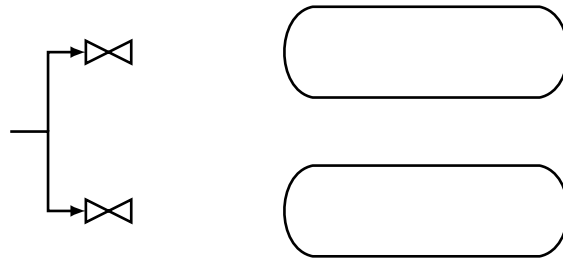
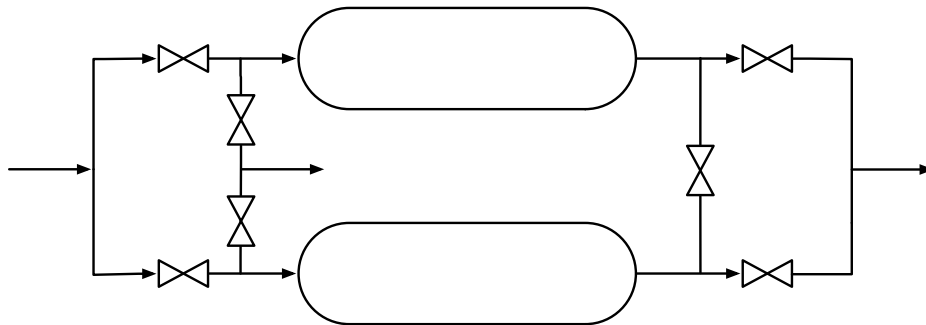Figure 2.3: Schematic representation of the PSA process.

Figure 2.4: Schematic representation of the PSA process.

recovered as desired products. The bottom and top streams from the HPC are made up of an oxygen rich liquid as well as liquid nitrogen. The liquid nitrogen stream is led though an heat exchanger an the fed as reflux into the top of the LPC. The bottom stream is, after heat integration, partially fed into the LPC as well as CAC. From the lower part of the LPC a side stream is drawn and led into the bottom of the CAC. At the same point the reflux from the CAC is fed back into the LPC [26].

2.2 Pressure swing adsorption

Pressure Swing Adsorption has been employed to separate gaseous mixtures for some time. During the 80's and 90's commercial applications for the production of oxygen or nitrogen have gained more and more attention. Especially the ability to construct very compact units the size of a briefcase, have led to the implementation of PSA processes for treatment of asthma patients or other medical appliances. But also larger scale plants have successfully been utilized, for example in the paper industry during the de-lignation of pulp. It remains true however, that for large scale industrial settings with high product quality demands, cryogenic separation remains the most viable alternative.

Separation is achieved during the PSA process by adsorption of one component in the mixture to a given bed. Once the bed is saturated with a the adsorbing species, it has to be regenerated in order to continue production. The ability to adsorb a certain species is dependent on the system pressure. At higher pressures more gas can be adsorbed then at lower pressures. Thus by reducing the pressure in the reaction vessel, the Adsorbent can be regenerated.

In order to avoid non-continuous processes, two or more reaction vessels are employed. Therefore the saturated vessel can be regenerated, while the other one continues production. By alternating
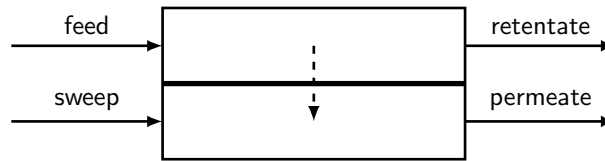
Figure 2.5: Membrane unit for gas permeation.

adsorption and regenerating in the different vessels continuous production can be achieved. A schematic for a simple two bed cycle is shown in fig. 2.4. Ambient air is first led through the first reaction vessel at the elevated pressure. Within the vessel nitrogen is adsorbed until saturation is reached. At that point the ambient air is led through the second vessel. A fraction of the product stream is fed into the first vessel and used as sweep for the regeneration of the adsorbent at lower pressure.

Depending on the size of the process two different pressure level are used. One cycle adsorbs the nitrogen at a pressure of approximately 7.5 bar while regeneration is done at ambient pressure. Within the alternative approach adsorption occurs under ambient condition, while for the regeneration step a vacuum pump reduces the vessel pressure. This process is the called Vacuum Pressure Swing Adsorption (VPSA).

An important role when designing the product is the choice of the adsorbent. For almost all current applications of PSA alumosilicates or zeolithes have been designed, tailored to the specific separation task. Their main advantages include a high selectivity towards a specic gas to be adsorbed as well as a very homogenous distribution of diameters in the molecular sieve.

2.3 Gas permeation

The separation of mixed gases by membrane process is called gas permeation. Its main strength in comparison with alternative processes are the low energy consumption and the possibility to produce flexible mobile units. As mentioned before it is not however capable of producing high quantity highly pure product streams. As fig. 2.1 illustrates the main application for the gas permeation process are small to moderate product streams at intermediate purities.

fig. 2.5 shows the schematic for a single stage membrane unit. Within the feed stream the gaseous mixture is fed into the unit, which can quickly be implemented. Within the unit one or more species migrate favorably through the membrane. In this case mostly dense polymer membranes are employed used. There have been some impressive results with metallic membranes, but due to the very high material costs they have not been adapted by the industry. Furthermore, since gaseous phases often have rather small molecular species, porous membranes cannot achieve desired separation. The driving force the separation process is a difference in partial pressure or species activity across the membrane. According to the molecular structure of each species, the structure of the separating membrane as well as the process parameters pressure and temperature, they permeate through the membrane in different quantities.

The process of permeation can be subdivided into three separate steps. Sorption at the membrane / feed interface, diffusion through the mostly dense polymer membrane and finally desorption at the

permeate side of the membrane.

2.4 Hybrid processes

The three different alternatives presented before constitute the major technologies for separations of gases and therefore the production of pure nitrogen and oxygen. All technologies have their specific advantages and disadvantages. As the separation of gases remains a major issue when facing upcoming challenges for our industries substantial efforts are being made to improve current processes in terms of ecological and economic performance. A very promising way to achieve such improvements to combine these technologies to form hybrid processes. Membranes offer many favourable characteristics are however rather limited when it comes to large flow-rates and high purities. When lower purities are required or the flow-rates are limited they offer however an efficient and cost effective way for gas separation. Therefore in the past years several alternatives for PSA - membrane [2] or membrane-cryogenic distillation processes [24] have been studied. The membrane can function within the process either as a pretreatment step, where an product enriched stream at medium purities and high flow-rates is produced, or after the main separation, when the main byproducts are already removed, as a last stage to reach very high purities.

3 Process design under uncertainty

For many real life decisions uncertainty plays a major role. As one might react differently to various scenarios that might occur in the future. In terms of process design two types of uncertainties can be distinguished. *Internal* and *external* uncertainties., where the internal ones refer to transfer-coefficients, diffusivities, efficiencies and other process parameters that cannot be exactly predetermined or that might change over time. External uncertainties denote all aspects that are not directly part of the process such as future prices for raw materials, energy, or the marketed product. In addition feed composition, pressures or ambient conditions are likely to change during process operations. All these factors will have an impact on operations and profitability of a given process.

The aim of the process design is to ensure feasibility for all possible realizations of the uncertain parameters. The naive way to account for such uncertainties is to find an optimal solution for nominal values of the uncertain parameters and then employ heuristic over design in the hope of maintaining feasibility and remain close to an optimal solution. However in practice this strategy will almost always fail to deliver an nearly optimal design [15].

Therefore several approaches have been developed to incorporate an rational approach to include flexibility in the design process. Ideally the design optimization would simultaneously recognize *feasibility*, *controllability*, *reliability* and *safety* in an multi-objective optimization. Although all the aspects stem from similar principles they differ considerably in their manifestation. While feasibility describes the mere possibility to operate a process under the defined conditions, controllability denotes wether those conditions can be reached from an initial starting point and gives a measure for quality and stability of the process in connection with the dynamic response to process disturbances.

Reliability and safety are qualities of a process that describe the consequences of unit failure on the operations of the process or the severity of those consequences with regard to how harmful they might be for personnel, environment or wildlife.

While all these aspects should be considered during the design phase it is questionable how well they all can be incorporated into a singe optimization scheme.

3.1 Earlier work

In its most general form the design problem for chemical processes can be written as:

$$\begin{aligned}
\underset{d,z}{\text{minimize}} \quad & C(d, z, x, \theta) \\
\text{subject to} \quad & h(d, z, x, \theta) = 0 \\
& g(d, z, x, \theta) \leq 0
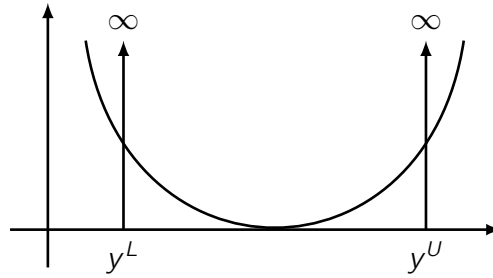\end{aligned} \tag{P 1}$$

Figure 3.1: test. [6]

Where d, z are the vectors for design and control variables respectively. The vector x contains all states specified by the physical process model and θ is comprised of all parameters subject to uncertainty. The aim of the program is therefore to identify the optimal set of design variables d for which by manipulating the control variables z feasible operations can be ensured for all possible realizations o the uncertain parameters θ.

Much research has been done within the field of process design under uncertainty that meet the requirements of optimal process design to different degrees. Most frequently used was the stochastic approach. If the probability distribution functions of all uncertain values is available, different minimization schemes can be employed. Kittrel and Watson [] thought the optimal design to be the one which minimizes the expected value of cost. Wen and Chang [] proposed a *relative sensitivity* of the cost – defined as fractional change in the cost function from its nominal value – and minimized either the expected value or the maximum probable value of this factional change. Other researcher included penalty functions to drive a solution away from constraint violations and then perform an unconstrained minimization or employ Monte Carlo simulation to find suitable over-design factors [] .

All the aforementioned approaches do not account for a fact derived from the actual application of the problem. In chemical processes, once a certain design is determined by the design variables d, the control variables z can still be adjusted to meet feasible operations once the uncertain parameters are realized. It is therefore advantageous to include this basic difference between the design and control variables in the mathematical formulation of the program. Again several different approaches have been studied. A summary of some of those can be found in [].

As mentioned before the main aim in terms of an design engineer when considering uncertainty must be to ensure feasible operations of a process for all or or the most likely realization of the uncertain parameters with the most attractive investment scheme.

4 Process economics

Aside from question wether a certain process is capable of producing products according to its specifications, it needs to be investigated if it does so in an economically viable manner. The modeling of process economics is a powerful tool to estimate project profitability. The evaluation of process economics has three major aims in the design phase.

- Compare design options with regard to profitability.

- Economically optimize a given design.

- Estimate project profitability

In any case the total cost of the project as well as the cash flow structure will have to be analyzed to supply an accurate estimate of the economic conditions. Furthermore an adequate measure to compare and analyze a project in economic terms needs to be employed.

The following sections will first describe how to estimate the total project cost in different stages of the design process. It is evident that, as the more information about a given process becomes available, the accuracy of any cost estimate will increase as well. During the design phase of a process roughly three different stages of cost estimation can be formulated.

- An estimate before designing the process yields an order of magnitude estimation for supporting market research efforts. Error $> 30\%$

- Estimate in the early design phase based on essential process equipment. Error $\pm 30\%$

- Estimate based on an advanced flowsheet and relevant process parameters. Error $\pm 20\%$

Once detail engineering commences, even more accurate calculations with errors reducing to $\pm 5\%$ can be undertaken[20]. At that point a concrete process option will have to be chosen and the investment decision will already have to be made. All optimization measures within the scope of this thesis will have concluded at that time.

Within sec. 4.1 first we will take a look at how the total cost of a chemical process might be estimated at different design stages. Subsequently in sec. 4.2 the different ways of evaluating a certain investment options and estimating a projects profitability will be discussed.

4.1 Project cost

An important factor in every given project is the total cost. During the design of a chemical process many important aspects of the future cost structure are unknown, as the final design is in development.

In general the total cost of implementing and operating a production site can be broken down into several subcategories.

- Battery limit investment

- Utility investment

- Off-Site investment

- Engineering fees

- Working capital

4.1.1 Before process design

Before any details about the process to be implemented are known, an estimate can only give an order of magnitude towards cost to be expected. The cost of the new process C_P can be related to the cost of a reference process C_P^0 by

$$C_P = C_P^0 \cdot \left(\frac{Q_P}{Q_P^0} \right)^x.$$ (4.1)

The degression coefficient x needs to be correlated from historical data.

As the overall price structure will change over time, the reference price will not reflect the current market situation. In order to adjust for that shortcoming several price indices are published all over the word. Some of those tailor to special branches of the industry, others give a picture of the price-development in a economy as a whole. The price ration of the prices at different times will then be equal to the ration of the price indices at the respective times

$$\frac{C_1}{C_2} = \frac{I_1}{I_2}.$$ (4.2)

For each index an somewhat arbitrary reference year is chosen. Among the most common indices are the Marshall & Swift index, the Nellson-Farrar-Index or the Chemical Engineering index. Some exemplary values for these indices are given in tab. 4.1. As one can see the development within the process industry very well matches the development in the economy as a whole, which is why for this rough estimate general indices should suffice.

4.1.2 During process design

Once the future design has been has been broken down to fewer potential options and first process flowsheets are available a more elaborate approach becomes possible.

	Marshall & Swift Installed Equipment Index 1926 ≡ 100		Nelson-Farrar Refinery Construction Index 1946 ≡ 100	Chemical Engineering Plant Cost Index 1957 ≡ 100
year	all industries	process industry		
1975	444	452	576	182
1980	560	675	823	261
1985	790	813	1074	325
1990	915	935	1226	358
1995	1027	1037	1392	381
2000	1089	1103	1542	394
2001	1093	1107	1565	396

Table 4.1: Price indices and their development.

Battery limit investment

The battery limit investment denotes all investments necessary to have all required equipment for process operations installed on-site. This includes structures necessary to house the process as well as delivery and installation of all individual assets. One major part of these cost will the the process equipment. As the exact manufacturers and models of the equipment will not be known in early design stages, an approach similar to the one in sec. 4.1.1 still needs to be employed. In contrast to before now the cost for individual pieces of process equipment will be considered separately. Each piece of equipment will have an specific feature that most influences its cost. For vessels and reactors this might be volume, while for heat exchangers the required heat exchange area is essential. The price for an piece of equipment i C_E^i can again be approximated by a simple power law

$$C_E^i = C_B^i \left(\frac{Q_E^i}{Q_B^i} \right)^{M^i} . \tag{4.3}$$

A reference price C_B^i is multiplied by the determining quantity Q^i normalized to a reference state Q_B^i and raised to the power M^i specific to each piece of equipment. Reference prices and quantities for various installations can be obtained from literature.

If information on the process conditions are available, they also can be considered in price calculations. Aside from the mere size of the equipment the process conditions will also have an affect on the expected cost. The predominant factors to that respect are pressure, temperature and the question wether corrosive or reactive media, which will require more resistant materials, will be present. Furthermore if a more detailed choice of process equipment is known this is considered as well. For example an plate-fin heat exchanger might be more expensive than a tubular model with the same heat-exchange area. In order to account for all those effect a form factor f_F is applied to the equipment cost

$$C_E^i = C_B^i \left(\frac{Q_E^i}{Q_B^i} \right)^{M^i} f_F^i = C_B^i \left(\frac{Q_E^i}{Q_B^i} \right)^{M^i} \underbrace{\left(1 + f_C^i + f_M^i + f_P^i + f_T^i \right)}_{=f_F^i} . \tag{4.4}$$

Where f_F denotes the form factor, f_C corrects for design complexity, f_M for material selection, f_P adjusts for extreme pressures and f_T for temperature.

As in the previous section all reference prices need to be corrected to compensate for the temporal price development, Here again the already discussed indices are used. Furthermore can regional changes in price structures be considered. Here again have correction factors to prices in an reference region in the world (e.g. USA) been published.

In addition to the purchased cost, the costs for installing the process equipment have an significant effect on the total needed investment of the process. These installation costs include:

- Installations costs

- Piping ,valves and electrical wiring

- Control system

- Structures and foundations

- Insulation and fire proofing

- Labour fees

Those again can be expressed as correction factors to the equipment price. Depending on the status of the information available they can be expressed as one unified factor or broken down to each specific category. One however needs to bare in mind, that costs for piping and valves – pieces of equipment in direct contact with process media – will be affected by the process conditions in a similar way as the actual equipment, whereas the other categories are more likely to remain unchanged. Thus attention needs to be paid, in with fashion the factors will be applied.

A word should be said to the cost for the control system. Most obtainable data will most likely refer to a decentralized control system, as it has been in use for many years. WIth ever more powerful computers a centralized approach, namely model predictive control (MPC) is becoming more relevant. As the structure for such a control system may vary significantly from the common designs, the cost factors may as well.

Services

The utility investments and off-site investments are often referred to as services. Therein included are all measures necessary to supply the process with the media required for operations. This includes but is not limited to generation and distribution of energy, steam, process gases. The utility investments in this context refer to all investments within the greater production site but out of the battery limits of the process. Off-site investments contain everything not contained in the site such as roads, power cables, communication systems or waste disposal. All these costs are expressed as fractions of the equipment cost at moderate temperature and pressure. This means, when applying these fractions, the factors f_M, f_P and f_T should not be considered at this point.

Once again in early design stages one has to resort to factors derived for statistical data, to calculate the cost of raw materials, energy and support media such as lubricants, heat or catalysts. If more detailed information on process streams is available the approach should be refined.

The cost of raw materials C_{RM} can then be calculated if the streams of individual raw materials m_i as well as their specific cost are known.

$$C_{RM} = \left(\sum_i^{N_{RM}} \dot{m}_i \cdot C_{RM}^i \right) \cdot t_{op}. \tag{4.5}$$

Much in the same way the cost for energy can be calculated. This is once more done for each individual pice of equipment, rather then for the whole process as it has been done for the raw materials. Hence with the needed energy for equipment i with respect to energy carrier j e_{ij} along with the price for energy carrier j C_{EC}^j the total energy cost C_{EC} can be assessed.

$$C_{EC} = \left(\sum_i^{N_E} \sum_j^{N_{EC}} \dot{e}_{ij} \cdot C_{EC}^i \right) \cdot t_{op}. \tag{4.6}$$

Working capital

The working capital includes all investments necessary for process operations. This means raw materials, payroll, extended credit to customers and so on. In contrast to all other costs the working capital can partially be retrieved when the process stops operations. How different types of cash flows, extended or owed credit should be handled will be disused in sec. 4.2. In addition to the cost of raw materials needed during process operations, which generate a product stream, raw materials are also needed to fill all vessels, reactors, columns and piping that male up the process. The cost of these needs to be considered as investment and not as operation cost, since more or less the same amount will remain bound until the process seizes operations and it can (partially) be retrieved.

$$C_{FILL} = \sum_i^{N_{RM}} V_i \cdot C_{RM}^i. \tag{4.7}$$

Total investment

When all contributions to the total investment are considered an estimate for the total price of the process can be calculated

$$C_P = \sum_i^{N_E} \left[C_B^i \left(\frac{Q^i}{Q_B^i} \right)^{M^i} \left(f_F \cdot f_{PIPE} + \sum_j f_j \right) \right] + C_{RM} + C_{EC} + C_{FILL} \tag{4.8}$$

It should be emphasized that in early design stages these calculations will at best yield an order of magnitude estimate for the expected cost of implementing a chemical process. Most literature sources give an accuracy of $\pm 30\%$ [20]. As the poject progresses more and more information becomes available an a more accurate estimate can be prepared. Those often rely on actual proposals from prospective manufacturers and suppliers.

4.2 Investment criteria

The total cost of a project its a very important measure to decide wether to undergo a certain endeavor. However in a complex financial system it cannot be taken as the sole factor to compare investment alternatives. Different other indices are used to measure the attractiveness of an investment. One main distinction can be made between different measurements. Those that work with averaged cash flows and consider the project as a singe time periods (sec. 4.2.1) and models that take into account cash flows made at different points in time – so called multi-period models (sec. 4.2.2).

4.2.1 Single period estimation methods

Among the most prominent single period methods are the payout time (POT) and the return of investment (ROI).

Payout time

Payout or amortization time is the time necessary to earn the total investment of the process. It is also often referred to as the break even point. A profitable venture will form that point on begin to make money. A shorter payback time is a measure for an more attractive investment.

$$POT = \frac{\text{capital expenditure}}{\text{incoming cash flow / period}} \qquad (4.9)$$

Return of investment

The return of investment is defined as

$$ROI = \frac{\text{average return / period}}{\text{capital expenditure}} \cdot 100\%. \qquad (4.10)$$

It denotes the equivalent to an interest rate if the earned interest is not reinvested such that the same Investment is considered in every period. The average return is calculated form the expected returns over certain duration of time. The time considered might either be the total lifecycle of the process or the expected write-off time. As capital expenditure most likely the total investment will be used. However it might give a more precise picture if write-off or the time of individual payments is considered when evaluating the capital expenditure.

4.2.2 Multi period estimation methods

As discussed earlier, when using only averaged values and considering only one time period, a distorted picture of the financial situation will evolve. The source of the money to be invested play a critical role in the evaluation process. Cash reserves, loans, preferred stock or other financial instruments are all viable sources of investment capital. Often a mixture of many different sources is used to allocate
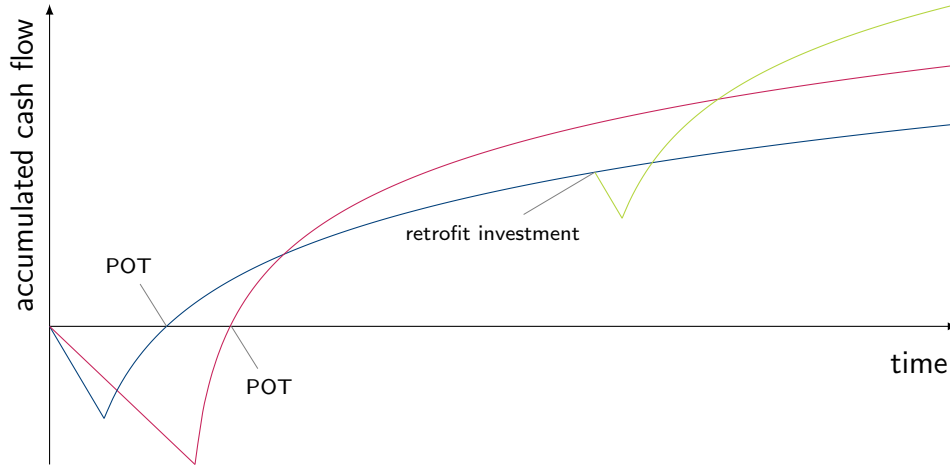
Figure 4.1: Accumulated cash flows over project life cycle.

all necessary funds. A generic structure of the cash-flows during the life-cycle of a given project is shown in fig. 4.1. When the project commences no revenue is generated and only investments are made. As process operations begin revenue is generated and the slope of the accumulated cash flow curve switches to an upward directions – assuming the project is profitable. As time progresses the produced product might reduce in value through competitors entering the market or other factors. When the curve intersects the abscissa the project investment is earned and the break point is reached. The two investment alternatives highlight that the amount of initial investment will affect the expected revenue. As more information is gathered during operations, opportunities may arise to optimize the process and leverage so far dormant potentials. These so called retrofit Investments would ideally lead to an improved cash flow structure as indicated by the green line.

Before further investigating multi-period model some basic ideas about financial mathematics and the treatment of interest should be reviewed. When investing the capital C_0 at compounded interest for n years at a rate of i %, the compound amount will yield

$$C_n = C_0 \cdot q^n. \tag{4.11}$$

Where q denotes the interest factor

$$q = 1 + \frac{i}{100}. \tag{4.12}$$

On the other hand the current value of an investment that will yield C_n in n years can be calculated by

$$C_0 = C_n \cdot q^{-n} \tag{4.13}$$

The above considerations always assume a single payment at the beginning or end of the entire period. Annuities however are usually in several trances with regular payments to be made or received at predefined instances. Assuming those payments are of equal size a, the final value can be computed by

$$C_n = a \cdot q^\alpha \cdot \frac{q^n - 1}{q - 1}, \tag{4.14}$$

while the current value of an annuity yields

$$C_0 = a \cdot q^{\alpha - n} \cdot \frac{q^n - 1}{q - 1}, \tag{4.15}$$

The factor α in the previous equations denotes wether payments are made at the beginning of a period ($\alpha = 1$ or at the end ($\alpha = 0$)

With that multi-period model can be discussed. Here not only different alternatives can be compared, but also the profitability in comparison with investments in financial products can be assessed.

Net present value

The net present value (NPV) describes the amount of money to be invested if all cash flows – incoming and outgoing – are discounted to the project start ($t = 0$). The present value of all expenses is then

$$C_{0e} = e_0 + e_1 \cdot q^{-1} + \cdots + e_n \cdot q^{-n} = \sum_i^n e_i \cdot q^{-i}. \tag{4.16}$$

Here it is given that all expenses are paid at the beginning of each period, as it is the most common case. If revenues r_i are realized then as well an equivalent formula would be attained. In most cases revenues will come in at the end of a period in which case the present value becomes

$$C_{0r} = r_0 \cdot q^{-1} + r_1 \cdot q^{-2} + \cdots + r_n \cdot q^{-(n+1)} = \sum_i^n r_i \cdot q^{-(i+1)}. \tag{4.17}$$

The NPV of a given project is then derived from the present values of all expenses and revenues

$$NPV = C_{0r} - C_{0e}. \tag{4.18}$$

For any project to be considered as investment alternative the present value needs to be positive since otherwise the investment would yield losses.

Discounted cash flow rate of return

The formula for the discounted cash flow rate of return is very similar to the one for a net present value. The difference is, that rather then computing the net present value with given interest rates, the present value is set to zero and the resulting interest rate its then calculated. Other than with the previous methods no analytical solution can be presented but rather an iterative approach to find a solution to

$$0 = \sum_i^n (r_i - e_i) \cdot q^{-i}. \tag{4.19}$$

Here its was assumed that all payments – incoming and outgoing – are made at the beginning of a period. The only variable is the interest rate which is included in the interest factors q. This methods gives the interest rate which would be necessary to earn all time dependent expenses within n years. In this case a higher $DCFRR$ indicates a more attractive investment.

Annuity method

Within the annuity method two different annuities are calculated and then compared. First the annuity a of an investment of C_0 at market conditions is of interest.

$$a = C_0 \cdot \frac{q^{n-\alpha}(q-1)}{q^n - 1} \tag{4.20}$$

This annuity is the amount that could be paid out each period if C_0 is invested, compound interest is considered and all funds are used up at the end of n years.

This is then compared to the annuity of the considered project

$$a_P = \sum_i^n (r_i - e_i) \cdot q^{-i} \cdot \frac{q^{n-\alpha}(q-1)}{q^n - 1}. \tag{4.21}$$

Only if $a_P > a$ is the project more profitable than simply investing the required capital in an financial product.

Interest Rates

With all the presented models its was implicitly assumed that interest rates for debit and credit are equal. The reality however is much different. It will therefore be prudent to use different rates of interest for each case. The basic calculations however remain unchanged. Especially the interest rate that can be earned when investing a certain amount will need to be estimated. As certain products with a know ROI will not necessarily be the most attractive options on the capital market. Thus in many companies there is an internal value given for this interest rate, which is calculated from historical data.

5 Mathematical process model

The industrial scale production of highly pure oxygen and nitrogen as well as noble gases is still carried out by means of the cryogenic process.

The initial process for production of pure oxygen first developed by Carl von Linde and first operated by Linde in 1902 [4] consisted of only a stripping section, in a way only half a rectification column. The reason for that is while it is easy to supply the heat necessary for the reboiler, a heat sink to operate a condenser at temperatures of about $95\ K$ is not readily available on our planet. due to that highly pure oxygen could be withdrawn from the bottom of the column, but nitrogen was only produces at mediocre purities.

The breakthrough that enabled operation of a "full" column, again developed by Linde in 1910, was to operate the column sections at different pressures. That way the energy needed in the reboiler could be withdrawn from the condenser of the other column half. This leads to a somewhat inverted construction of the tower in comparison to regular distillation units, because the lower section forms the top section in this case and condenser and reboiler usually at the top and bottom of a column are combined in a single heat exchange unit in the middle of the column. This specialty of the process also leads to the need that the absolute values of the energies used in condenser and reboiler need to be equal. On terms of modelling the process this also forms a considerable challenge.

A simplified overview of the major process steps is given in fig. 5.1. Within the following sections the different process steps will be discussed in more detail. When appropriate the mathematical model for single process units is discussed as well. In addition to the separate process steps displayed in fig. 5.1 the aspect of heat integration os essential to successfully operating an air separation unit (ASU). This aspect will be discussed separately as well (sec. 5.3)

The pre-purification step of the process aim to reduce the amount of unwanted impurities from the ambient air as far as possible. The main sources of contamination are in this case dust and other organic components that can be found depending on the time of year and location of the plant. Furthermore are water and carbon dioxide common components in ambient air. The removal of these components is undertaken by means of adsorption molecular sieves such as zeolite or for initial steps coarser sieves. However the design and simulation of these pre-purification measures is not within the scope of this work. For more information the interested reader is referred to [1].
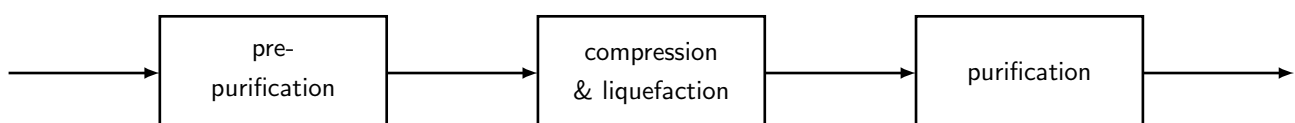
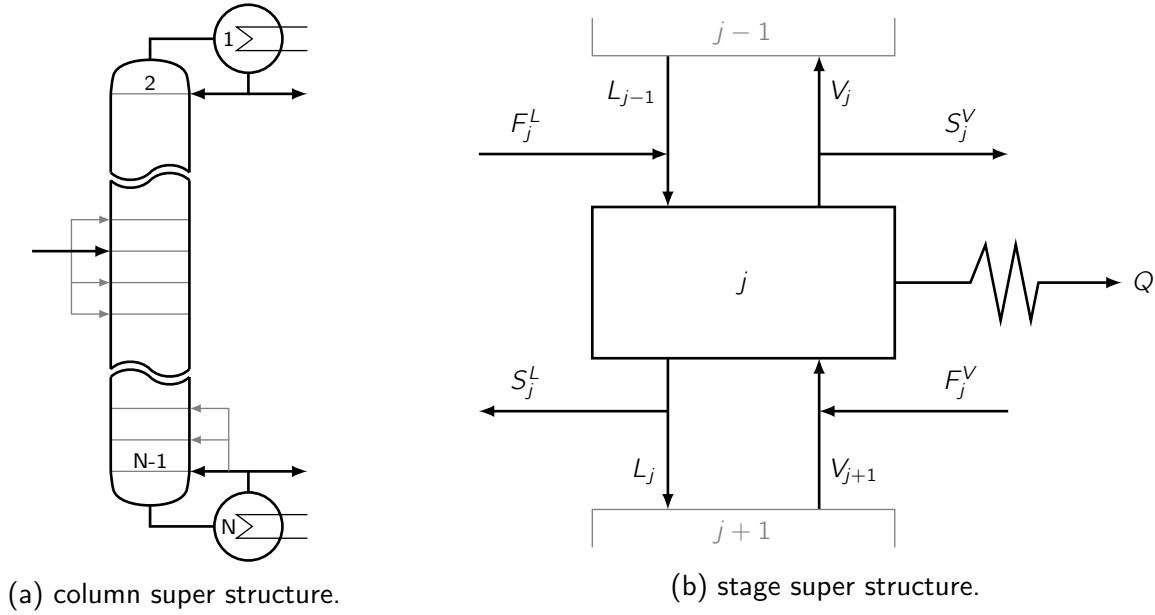Figure 5.1: simplified cryogenic air separation process.

(a) column super structure.

(b) stage super structure.

Figure 5.2: superstructures for column and column stages.

5.1 Purification

The purification of the liquefied gases is performed by distillation columns operated at different pressure. These distillation columns form the heart of the air separation process and their operation parameters are crucial in terms of enabling the desired separation. While the aspect of heat integration poses is also essential in terms of profitability of the process.

Subsequently this section is concerned with the description of different aspects of modeling distillation columns. First the mathematical model will be presented in more detail. Afterwards the handling of different specifications for individual columns is elaborated upon. Lastly the issue of initializing the respective models and the implemented solution is presented.

5.1.1 Distillation column model

In this section the working equations used to model the different distillation columns in the process, known as the MESH equations, are given. These equations, although rather plain at first glimpse, form a set of highly non-linear, highly coupled equations. The solutions of these equations is not a trivial task for current solution algorithms, whose success is highly dependent on the quality of initial guesses provided. Therefore a strategy used for the automated generation of such guesses will be described as well.

Fig. 5.2a and fig. 5.2b show the super structures for a distillation column with a single feed and and no side draws and an inner column stage. The acronym MESH stands for Material (M), Equilibrium (E), Summation (S) and Enthalpy (H) equations which are given below.

Material balances The material balances in their most general form for an inner column stage can be written as

$$0 = \left(V_j + S_j^V\right) \cdot y_{i,j} + \left(L_j + S_j^L\right) \cdot x_{i,j} - V_{j+1} \cdot y_{i,j+1} - L_{j-1} \cdot x_{i,j-1}$$
$$- F_j^V \cdot z_{i,j}^V - F_j^L \cdot z_{i,j}^L, \qquad i = 1 \ldots n_C \quad j = 1 \ldots N. \quad (5.1)$$

Here the vapour and liquid phase of the feed to the stage are considered separately. While this is not strictly necessary is allows for certain freedoms in terms of modelling column operations, as sometimes the vapour fraction of a given feed is actually fed into the vapour phase of a stage and therefore effectively in the liquid phase of the stage above.

To facilitate convergence the side draw streams S_j^V and S_j^L are made dimensionless by means of the respective vapour and liquid flows on that stage to form the vapour

$$s_j^V = \frac{S_j^V}{V_j}, \qquad j = 1 \ldots N \quad (5.2)$$

and liquid

$$s_j^L = \frac{S_j^L}{L_j}, \qquad j = 1 \ldots N \quad (5.3)$$

stripping factors. Replacing the side-streams in the material balances by their corresponding stripping factors yields

$$0 = \left(1 + s_j^V\right) \cdot V_j \cdot y_{i,j} + \left(1 + s_j^L\right) \cdot L_j \cdot x_{i,j} - V_{j+1} \cdot y_{i,j+1} - L_{j-1} \cdot x_{i,j-1}$$
$$- F_j^V \cdot z_{i,j}^V - F_j^L \cdot z_{i,j}^L, \qquad i = 1 \ldots C, \quad j = 1 \ldots N. \quad (5.4)$$

As the model is also to be used for optimization purposes further extensions are necessary. The location of individual feeds as well as the number of theoretical or real stages of the column is to be optimized. To accommodate that need, new variables need, namely the feed split ζ_{ij}^F for feed i to stage j as employed by [11] are introduced. The split variables are integer variables that can take a value of 0 or 1. Additionally it is assumed that each feed will only be fed to a single stage thus

$$0 = 1 - \sum_{j=1}^{N} \zeta_{ij}, \qquad i = 1 \ldots F, \quad j = 1 \ldots N, \quad (5.5)$$

where F denotes the number of feeds, comprised of vapour (F^V) and liquid F^L feeds.

In order to optimize the number of stages several superstructures are possible. One can optimize the reboiler reflux location and condenser reflux location or each single one along with the feed and side draw locations. The stage number is then changed as all stages between condenser or reboiler reflux are effectively rendered inactive. The solution of the mass and energy balances for each respective stages becomes trivial as only one single vapour or liquid stream enters and exits the stage. While

the choice if condenser and or reboiler reflux is optimized is somewhat arbitrary some studies have shown [14] that the strategy of optimizing only feed location and reboiler reflux location possesses some numerical advantages in terms of performance of the solution algorithm.

With the newly introduced split variables for liquid ζ_{ij}^L and vapour ζ_{ij}^V as well as the reboiler reflux ζ_j^R and the liquid ζ_{ij}^{SL} and vapour ζ_{ij}^{SV} side draws, the material balances can be written as

$$
\begin{aligned}
0 = \left(1 + s_j^V\right) \cdot V_j \cdot y_{i,j} + \left(1 + s_j^L\right) \cdot L_j \cdot x_{i,j} - V_{j+1} \cdot y_{i,j+1} \\
- L_{j-1} \cdot x_{i,j-1} - \sum_{k=1}^{F^V} \zeta_{kj} \cdot F_j^V \cdot z_{i,j}^V - \sum_{l=1}^{F^L} \zeta_{lj} \cdot F_j^L \cdot z_{i,j}^L - \zeta_j^R \cdot V_N \cdot y_{iN}, \\
i = 1 \ldots C, \quad j = 1 \ldots N, \quad k = 1 \ldots F^V, \quad l = 1 \ldots F^L.
\end{aligned} \tag{5.6}
$$

Furthermore to be able to optimize side draws, the stripping factors have to be reformulated accordingly

$$
s_j^V = \frac{\sum_{i=1}^{S^V} \zeta_{ij}^{SV} S_j^V}{V_j}, \qquad j = 1 \ldots N, \quad i = 1 \ldots S^V, \tag{5.7}
$$

$$
s_j^V = \frac{\sum_{i=1}^{S^L} \zeta_{ij}^{SL} S_j^L}{L_j}, \qquad j = 1 \ldots N, \quad i = 1 \ldots S^L. \tag{5.8}
$$

Equilibrium equations   The equilibrium equations are given by

$$
y_{ij} = K_{ij} \cdot x_{ij}, \qquad i = 1 \ldots C, \quad j = 1 \ldots N. \tag{5.9}
$$

Where the equilibrium ratio K_{ij} is computed from the relations that describe a vapour liquid equilibrium (VLE).

A vapour and liquid phase are in equilibrium, when the fugacities in the vapour f_i^V and liquid f_i^L phase for each species i are equal [3]

$$
f_i^V = f_i^L, \qquad i = 1 \ldots n_C. \tag{5.10}
$$

This can also be written in terms of the, liquid activity coefficient γ_i, the pointing factor F_{Pi}, the reference vapour fugacity coefficient φ_i, the vapour pressure p_i^S as well as the system pressure p along with the vapour and liquid molar fractions

$$
\gamma_i \, F_{Pi} \, \varphi_i^0 \, p_i^S \, x_i = \varphi_i \, p \, y_i, \qquad i = 1 \ldots n_C. \tag{5.11}
$$

(a) condenser stage.   (b) reboiler stage.
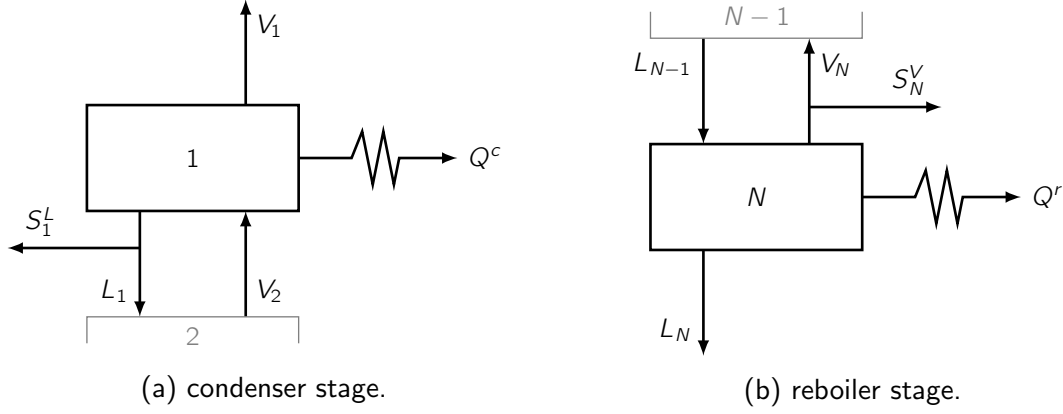
By reformulating eq. (5.12) an expression for the equilibrium ratios can be derived

$$y_i = \underbrace{\frac{\gamma_i \, F_{Pi} \, \varphi_i^0 \, p_i^S}{\varphi_i \, p}}_{K_i} x_i, \qquad i = 1 \ldots n_C. \tag{5.12}$$

The equations to determine the quantities used when computing the equilibrium ratios are by themselves functions of temperature, pressure, and vapour as well as liquid molar fractions. They are further discussed in sec. 5.4. It therefore becomes evident that the equilibrium ratios are a major source non-linearities in the MESH equations.

Enthalpy balances The enthalpy balances can again be written using the previously defined stripping factors and splitting variables

$$0 = \left(1 + s_j^V\right) \cdot V_j \cdot h_j^V + \left(1 + s_j^L\right) \cdot L_j \cdot h_j^L - V_{j+1} \cdot h_{j+1}^V$$
$$- L_{j-1} \cdot h_{j-1}^L - \sum_{k=1}^{F^V} \zeta_{kj} \cdot F_k^V \cdot h_j^{FV} - \sum_{l=1}^{F^L} \zeta_{lj} \cdot F_j^L \cdot h_j^{FL} - \zeta_j^R \cdot V_N \cdot h_N^V,$$
$$i = 1 \ldots C, \quad j = 1 \ldots N, \quad k = 1 \ldots F^V, \quad l = 1 \ldots F^L. \tag{5.13}$$

Condenser and reboiler Condenser and reboiler are modeled more or less as regular column stages. However they possess certain specialties that are explicitly considered in the column model. For one it is assumed that no feeds enter the reboiler and condenser stage. Furthermore no vapour side stream is drawn from the condenser stage and no liquid side stream from the reboiler stage.

Additionally the condenser stage needs to examined a little further. In terms of operations several assumptions can be made for the condenser. In general one can distinguish a total, partial vapour and partial vapour liquid condenser. For the total condenser all vapour that enters the respective stage is condensed and only liquid product is drawn (here modeled as a side draw). The partial vapour condenser condenses only the vapour the is fed back into the column and all product that is drawn is gaseous. The partial vapour liquid condenser denotes the most general case, where part of

the incoming vapour is condensed and product ist drawn as vapour and liquid. The most important thing to consider in these different cases, is that while in both partial condensers a vapour liquid equilibrium takes place, due to the absence of vapour the same does not hold for the total condenser. To accommodate that fact the MESH equations have to be adjusted [19]. While the material and energy balances remain unchanged the equilibrium equations have to be altered. First the vapour and liquid compositions are set equal for all but one component

$$x_{i1} = y_{i1} \qquad i = 1 \ldots C - 1,\tag{5.14}$$

and the condenser temperature is determined by the bubble point equation

$$0 = 1 - \sum_i K_{i1} \cdot x_{i1} \qquad i = 1 \ldots n_C.\tag{5.15}$$

When implementing the model in a process simulator it is sensible to consider, that due to the limited accuracy of computers the omitted component in eq. (5.14) needs to a non-trace component in the condenser stage. The implemented model therefore as to specify such a component when a total condenser is chosen to avoid numerical difficulties.

In practice it is highly unlikely, that the exact amount of energy required to condensate all liquid will be drawn from the condenser. More likely, if all vapour is condensed, a little more energy will be withdrawn and slightly sub-cooled liquid will leave the condenser. Therefore the model includes the possibility to specify a degree of sub-cooling T^{sub} which will be considered when calculating the equilibrium ratios.

Pressure profile For a steady-state model the pressure profile of a column would usually be specified. However as it is inconvenient and unpractical to specify a pressure for each stage one might either specify a pressure at the top and bottom stage and assume a uniform pressure profile along the column, or specify either top p_1 or bottom pressure p_N along with a total pressure drop Δp, or a stage-wise one Δp_{stage}. However the issue is further complicated if one considers the case of optimization for number of trays. In that case several trays will become inactive. For those trays the mass and energy balances become trivial, as only liquid enters and exits these trays. (For tÂ´he case employed here, where the reboiler reflux is being optimized). This also means, that from the last active tray down to the reboiler – if present – there should be a uniform profile. however, if a uniform pressure profile from that stage down is not enforced, the solver will have to compensate for slight changes in the equilibrium due to pressure variations with minimal vapour flow-rates. This is very undesirable, as it might to lead to severe problems in the solver, or the calculation of other properties, dependent on these values. To account for this issue, the reboiler reflux split can once more be employed

$$p_i = p_{j-1} + \left(1 - \sum_{k=1}^{j-1} \zeta_k^R \right) \cdot \Delta p_{j-1} \qquad j = 1 \ldots N.\tag{5.16}$$

As an alternative to specifying the pressure, one might consider calculating the pressure drop form (semi)-empirical models. There a numerous correlations for different types of column internals. These

correlations become particularly important id column dynamics are to be considered, as they make a connection between holdups and flow-rates within the column. Two different pressure drop models have been implemented, one for trayed columns and another one for structured packings. As they are closely tied to dynamics, they will be discussed in closed detail in sec. 6.

5.1.2 Specifications

The equation systems presented above is comprised of NC component balances, NC equilibrium equations, $2N$ summation equations and N energy balances. This gives a total of $N(2C + 3)$ equations. On the other hand there are N temperatures and pressures, $2N$ molar flow rates, N energy streams, and NC vapour as well as and liquid concentrations. Additionally the feed flow rates compositions and temperatures and the side draw split fractions or flow rates appear as variables. The feeds and side draws would usually be specified, which leaves a total of $N(2C + 5)$ variables.

The pressure profile of a distillation column is usually specified. Either by explicitly assigning a given pressure to each stage, or more conveniently by defining a pressure either the top or bottom pressure as well as the pressure drop per stage

$$\Delta p_{stage} = p_i - p_{i-1}, \qquad i = 2 \ldots N. \tag{5.17}$$

In terms of unit operations this pressure drop is of high significance, as many columns can only be feasibly operated, if the pressure drop does not exceed certain limits. In case of the ASU the production of Argon only became feasible as structured packings, which display a very low pressure drop, became available. This is due to the large number of theoretical stages required to attain the desired Argon purities.

The energies Q_i denote addition heaters or cooler on the respective stages. For all intermediate stages these values would be specified as well. If all energies would be specified, that would – along with the pressure profile – sum up to $2N$ specifications, which leaves $N(2C + 3)$ unknowns. As the number of equations and unknowns are the equal, this system can them be solved.

In practice it is often challenging to correctly guess the condenser and reboiler heat loads in advance. This is especially true since they have a tremendous impact on the overall performance of the column. Hence it is often desirable to supply other specifications than the respective heat loads. To allow for such specification so called discrepancy functions can be introduced [16], which replace the energy balance for the condenser and / or reboiler stage.

One common specification is the so called reflux ratio $\nu^D = \frac{L_1}{V_1 + S_1^L}$ for the condenser, or the boilup ratio $\nu^R = \frac{L_N}{V_N}$ for the reboiler. They are defined as the ratio of the molar flowrate sent back into the column over the product flowrate which leaves the column. For the reboiler this denotes a liquid stream, while for the condenser the product can be gaseous and liquid. Specifying this leads to

$$0 = L_1 - \nu^D \cdot (V_1 + S_1^L), \tag{5.18}$$
$$0 = V_N - \nu^R \cdot L_N, \tag{5.19}$$

as discrepancy functions. I addition to that further specifications are conceivable. Most commonly distillate (D) or bottoms (B) flow rates, or purities, component flow rates (d_i, b_i) or temperatures. The corresponding discrepancy functions are summarized in tab. 5.1.

specification	replacement for H_1	replacement for H_N
reflux or boilup ratio	$0 = L_1 - \nu^D \cdot (V_1 + S_1^L)$	$0 = V_N - \nu^R \cdot L_N$
temperature	$0 = T_1 - T_{spec}$	$0 = T_N - T_{spec}$
product flowrate	$0 = (V_1 + S_1^L) - D$	$0 = L_N - B$
component product flowrate		$0 = L_N \cdot x_{iN} - b_i$
mole fraction	$0 = y_{i1} - y_{i,spec}$	$0 = x_{iN} - x_{ispec}$

Table 5.1: discrepancy functions for different column specifications.

The specifications for the reboiler stage are quite straightforward, in contrast to that, different cases for the condenser have to be considered. In the most general case the top product can be drawn as vapour and liquid. This case is here called a partial vapour liquid condenser. The other cases are a total condenser, where all the vapour entering the condenser stage is condensed, and all product is drawn as a liquid stream, as well as a partial vapour condenser, where only the reflux is condensed and all product is drawn as vapour. As discussed earlier no VLE takes place in the condenser stage, if a total condenser is specified, which needs to be accounted for. Both the total and partial vapour condensed implicitly include an extra specification since in former case the top vapour product flow rate becomes zero and in the latter the top liquid product flowrate. Furthermore a specification of the condenser energy is infeasible as well as implicitly given for the total condenser. In case of the partial vapour liquid condenser no implicit specification is given, which requires an additional specification. In general two top specifications are necessary, whereas only one bottom specification is required. These top specification can include the condenser duty, any top flowrate, the reflux ratio as well as a newly introduced quantity, the top vapour fraction defined as

$$\nu^{vap} = \frac{V_1}{V_1 + S_1^L}. \tag{5.20}$$

5.1.3 Column initialization

As mentioned before the solution of the MESH equations can pose a considerable problem to numerical solvers. It is therefore necessary to supply the solver with feasible estimates for the involved variables that can be used as an initial guess to facilitate convergence of the process model. A lot of effort has been spend to formulate robust strategies to initialize distillation column models. One of the most prominent is the so called Inside-Out algorithm first introduced by Boston and Sullivan [7]. Within this algorithm an inner and outer iterative loop are employed. Within the outer loop approximate parameters for simplified models of phase equilibrium and enthalpy are computed by rigorous thermodynamic models and guesses for stage temperatures and concentrations. Within the inner loop new stage temperatures and concentrations are by solving the MESH equations using the simplified thermodynamic models. Once the inner loop converges the simplified model parameters are updated within the outer loop by means of the newly calculated temperatures and concentrations. This algorithm converges in many cases even for very poor initial guesses and has been extended to handle complex columns with side-draws and even reactive distillation [8]. It is still in use in the process simulator Aspen Plus® . However as it is used within an modular algorithmic environment it is not applicable to equation based simulators such as gPROMS® .

More recently other approaches have been published to attain improved initial guesses. Fletcher and Morton [13] proposed the solution of a column model at infinite reflux and zero feed flow rate. This leads to a much simplified model which can be solved more easily. The computed purities and stage numbers can give valuable insight into the process model. As this approach relies on the solution of a simplified model and has no algorithmic elements, it can be implemented in equation based process simulators.

Another strategy that has been successfully applied to zeotropic and azeotropic mixtures relies on solving the column model for the limiting case of the adiabatic column [5]. The adiabatic column in this case is the column with the minimal entropy production in a real column. To avoid entropy production all streams that come in contact must be in equilibrium. To achieve this the column would have to employ an infinite number of stages and have an infinite number of heat exchangers along its length. The adiabatic column then uses only two heat exchanger in the condenser and reboiler stage and assumes a pinch point at the feed stage.

Furthermore a much simpler approach has proven adequate for many applications [16] which is also employed as a starting point in this work. There feed properties are used as initial guesses. First a linear temperature profile form the boiling temperature to dew temperature of the feed is used to initialize temperatures, whereas a simple flash at average column pressure and feed temperature yields a vapour and liquid concentration that which is used as uniform profile for every column stage. However as the feed might be sub-cooled liquid or super-heated vapour the TP-Flash is replaced by a specified vapour fraction. As vapour fraction for the flash initial estimates of the vapour and liquid flow rates at the top and bottom of the column are used. The stage-wise molar flow-rates are computed from the constant molal overflow assumption.

While this approach leads to model convergence in many cases, it is not entirely robust. While the system considered in this case displays only moderate non-idealities it is highly cupeled. Especially the low pressure column (LPC) has multiple feeds and side draws, which leads to non-convergence if the aforementioned initialization strategy is employed. However the fact that the system is not highly non-ideal can be exploited. Whenever the K-values are not too much dependent on mixture composition an intermediate step can be used to refine concentration guesses. The constant molal overflow assumption is retained and the equilibrium ratios are computed based on the initial guesses from the first stage. The component balance is then reformulated only in terms of liquid component flow-rates l_{ij}

$$0 = \left((1 + s_j^V) \cdot K_{ij} \cdot \frac{V_j}{L_j} + (1 + s_j^L) \right) \cdot l_{ij} - \frac{V_{j+1}}{L_{j+1}} \cdot K_{ij+1} \cdot l_{ij+1} - l_{ij-1}$$
$$- F_j^V \cdot z_{i,j}^V - F_j^L \cdot z_{i,j}^L, \qquad i = 1 \ldots C, \quad j = 1 \ldots N. \quad (5.21)$$

eq. (5.21) is linear in the liquid component flow rates. Furthermore vapour component flow rates are substituted in the linear component balance and can be computed by

$$0 = v_{ij} - K_{ij} \cdot \frac{V_j}{L_j} \cdot l_{ij} \qquad i = 1 \ldots C, \quad j = 1 \ldots N. \qquad (5.22)$$

On of the reasons eq. (5.21) is formulated in terms of component flow rates rather than molar fractions, is that the molar fraction computed in that manner would not be normalized. If the mole fractions are computed from the component flow rates normalization is implicitly given

$$x_{ij} = \frac{l_{ij}}{\sum_k^C l_{kj}} \qquad i = 1\ldots C, \quad j = 1\ldots N. \tag{5.23}$$

$$y_{ij} = \frac{v_{ij}}{\sum_k^C v_{kj}} \qquad i = 1\ldots C, \quad j = 1\ldots N. \tag{5.24}$$

The total molar flow rates used in eq. (5.21) are computed by solving stage-wise total mass balances under the constant molal overflow assumption. This assumption postulates that the heat of vaporization is independent of system composition. Therefore always the same amount of liquid enters and leaves a given stage

$$0 = L_j + S_j^L - L_{j-1} - (1 + q_F^L) \cdot F_j^L - q_F^V \cdot F_j^V \qquad j = 1\ldots N. \tag{5.25}$$

Only at feed and side draw stages the total flow rates change. To introduce some more accuracy to the model, the available information about the feed is considered. When a feed enters as super-heated vapour or sub-cooled liquid, it has the capability to evaporate some liquid or liquefy some vapour. To account for that fact the feed energy parameters q_F^L and q_F^V are introduced

$$q_i^{FV} = \frac{H_i^{FV} - H_i^V}{H_i^V - H_i^L}, \qquad i = 1\ldots F^V, \tag{5.26}$$

$$q_i^{FL} = \frac{H_i^{FL} - H_i^L}{H_i^V - H_i^L}, \qquad i = 1\ldots F^L. \tag{5.27}$$

The vapour total flow rates are then computed from the total mass balances

$$0 = L_j + S_j^L + V_j + S_j^V - L_{j-1} - V_{j+1} - F_j^L - F_j^V, \qquad j = 1\ldots N. \tag{5.28}$$

As no energy balances are included at this stage, the condenser and reboiler stage are characterized by the reflux ($\nu^c = \frac{V_1}{L_1}$) or boilup ratio ($\nu^r = \frac{V_N}{L_N}$) respectively. This leads to

$$0 = V_1 - \nu^c \cdot L_1, \tag{5.29}$$
$$0 = L_N - \nu^r \cdot V_N. \tag{5.30}$$

To close the equation system the global mass balance is included

$$0 = V_1 + L_N + \sum_{j=1}^N (S_j^V + S_j^L - F_j^V - F_j^L), \qquad j = 1\ldots N. \tag{5.31}$$

Figure 5.3: example
column.
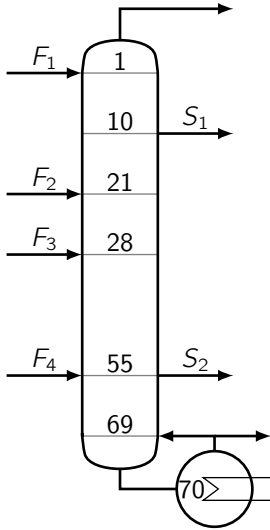
feed specifications

stream	flow $[\frac{kmol}{hr}]$	$z_{O_2}[-]$	$z_{N_2}[-]$	$z_{Ar}[-]$	$T[K]$	$p[bar]$
F_1	2985.77	4.674E-10	0.9999	6.378E-7	79.45	1.3
F_2	1836.36	0.2095	0.7812	0.0093	98.91	1.3
F_3	7609.06	0.2920	0.6950	0.0130	81.88	1.3
F_4	774.94	0.9161	5.393E-12	8.394E-2	92.13	1.8

column specifications

stages	S_1 frac	S_2 frac	boilup ratio	p^{top}	p^{bot}
70	10	0.15	3.5	1.2 bar	1.3 bar

Table 5.2: column specifications.

Init specification

At this point it should be mentioned, that not all specifications are compatible with the initialization procedure. As no energy balances are solved during initialization, specified condenser or reboiler duties cannot be considered in this stage. Furthermore purity specifications are also not applicable during this stage, they are computed by a different approach. Due to that it is necessary – when duties or purities are specified – to supply substitute specifications, that can be used during initialization. Essentially all specifications concerning top and bottom flow rates and flow ratios are usable during initialization. The user interface implemented specifically asks for substitute specifications if any aforementioned cases are encountered.

Example

To illustrate how the initialization procedure works an example has been constructed of a rather complex column – or column section – with multiple feeds and side draws (fig. 5.2). It is taken from an example process of cryogenic air separation. The column in question is a column section without an condenser stage and displayed the most difficulties in terms of convergence when constructing the process flowsheet.

In addition to the aforemention initialization strategy, columns with side draws present are handled in a slightly different manner. Initially the side draws are disregarded. Then the initialization procedure is carried out. Once the column without side draws has converged, a homotopy approach

$$f(\mathbf{x}) = (1 - \alpha) \cdot f_0(\mathbf{x}) + \alpha \cdot f_1(\mathbf{x}) \tag{5.32}$$

is employed, where the parameter α is initially set to zero and then gradually moved to a value of one. During the initialization homotopies could generally be employed to move from one step to another. While in some cases robustness is improved by such a strategy, it is always computationally far more expensive then simply jumping between different stages.
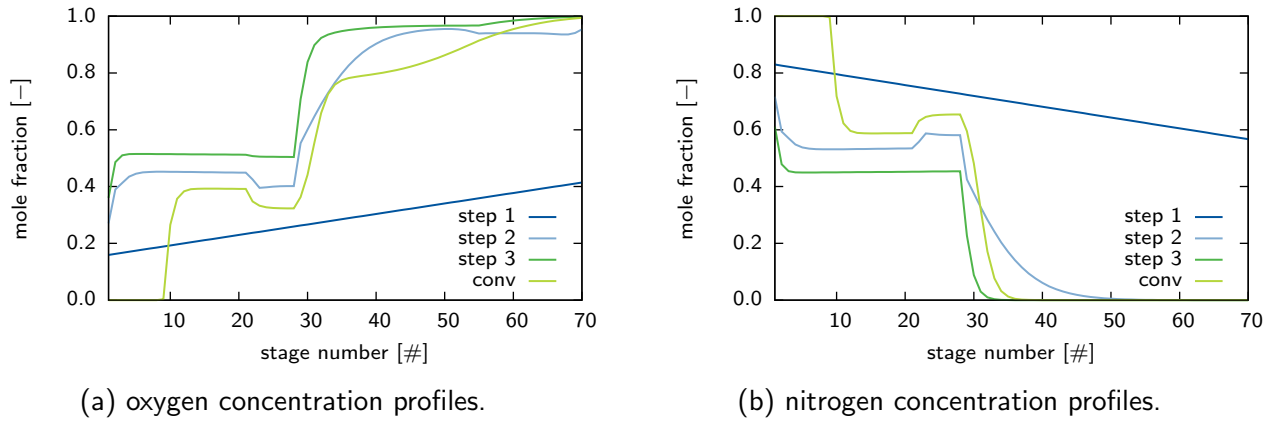
(a) oxygen concentration profiles.

(b) nitrogen concentration profiles.

Figure 5.4: initialization example concentration profiles.

For clarity reasons the different steps of the initializations procedure a repeated in a tabular manner

1.
   - linear temperature profile between dew (T^{dew}) and bubble point temperature (T^{bub}) of mixed feed.
   - linear profile between feed flash vapour and liquid compositions for liquid stage compositions.
   - constant profile for vapour compositions.
   - molar flow rates from constant molar overflow model.
   - side draw flow rates set to zero.

2.
   - total molar flow rates form constant molar overflow model.
   - simplified equilibrium ratios from initial liquid mole fractions and linear temperature profile.
   - liquid and vapour mole fractions from linearized mass balances.

3. rigorous solution of MESH equations with side draws still set to zero.

4. homotopic approach to MESH equations with side draws considered.

The resulting profiles for oxygen and nitrogen concentrations in the example column can be seen in fig. 5.4a and fig. 5.4b.

5.2 Compression & liquefaction

The issue of cooling the ambient air to process temperatures at around 90 K is not an easy one. The main hindrance is, that a heat sink at this temperature level is not readily available. Lucky thermodynamics offer a different way to reach such temperatures. In order to do so, the ambient air first needs to be compressed and then expanded again. Cooling then occurs by either exploiting the *Joule-Thompson* effect or isentropic expansion. First a few comments are made about the compression stage, while afterwards the governing principles for cooling by expansion will be described.
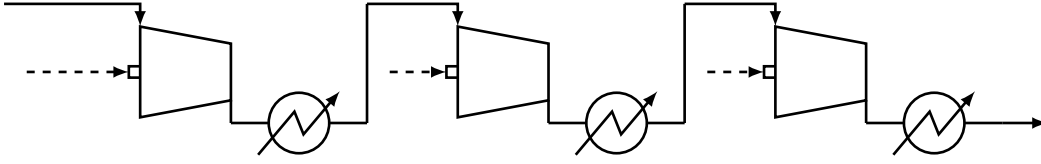
30

Multi-stage compression

Figure 5.5: Multi-stage compression.

Compressors and expanders are among the most common process equipment. A multitude of processes utilizes them as primary or auxiliary units. While the tasks performed by especially the compressors is essential for reaching the required process temperatures, they have less impact in terms of process performance and capital expenditure.

The rigorous modeling of continuous flow machines in terms of unit operations poses great challenges. For specific units it may be undertaken by means of CFD simulations or employing characteristics diagrams, which require extensive experiments and can usually be obtained from the manufacturer. For the purposes of process design however a simpler approach with unit efficiencies is appropriate.

In order to attain the desired compression it is beneficial, to use a multi stage compressor with inter-cooling as depicted in fig. 5.5. This yields a lower energy consumption as a single stage unit for the same compression ratio.

Cooling by expansion

The liquefaction of gases requires temperatures well below ambient conditions. In order to reach such conditions one cannot utilize natural occurring coolants, but rather cooling effects that occur during the expansion of compressed gases. First we consider the expansion through an expansion valve or so called *Joule-Thompson* - valve. If we assume very good insulation of conditions this expansion can closely be approximated by an isenthalpic process ($h_1 = h_2$). To describe the change in temperature during isenthalpic expansion the *Joule-Thompson* coefficient

$$\mu_{JT} = \left(\frac{\partial T}{\partial p}\right)_h,$$
(5.33)

which denotes pressure derivative of the temperature at constant enthalpy can be considered. This can be transformed into

$$\mu_{JT} = \frac{1}{c_p}\left[T\left(\frac{\partial v}{\partial T}\right)_p - v\right]$$
(5.34)

If we employ the Peng-Robinson equation of state we can plot the isenthalpes for ambient air ($x_{N_2} = 0.7812$, $x_{O_2} = 0.2095$, $x_{Ar} = 0.0093$) in a PT-diagramm (fig. 5.6). One can easily see, that in certain ranges a pressure decrease will result in an increase in temperature, while for other regions in a decrease. It is interesting to mention that the non-idealities of a given gas give rise to this effect. For an ideal gas the temperature change at isenthalpic expansion would always be zero. Luckily for
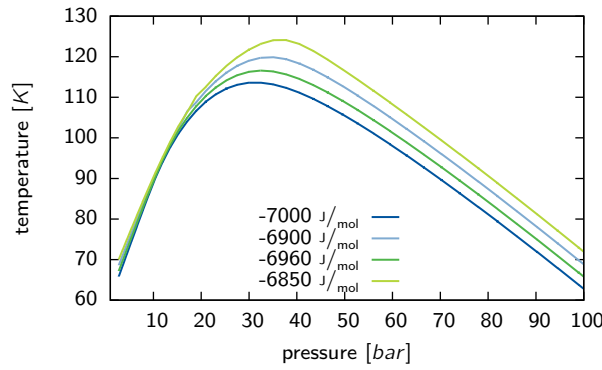
Figure 5.6: Isenthalpes computed by Peng-Robinson model.

the cryogenic engineer real gases deviate from ideal behaviour especially at elevated pressures and low temperatures. It is therefore important to give some consideration to the thermodynamic model used to describe the properties of the system in question, as the non-ideal properties need to be captured appropriately.

A different way of expanding a compressed gas, is by letting it produce work in an fluid kinetic machine. If one assumes an adiabatic devices and disregards irreversible effects, this process can be viewed as isentropic. Analogous to the isenthalpic case an isentropic expansion coefficient can be defined

$$\mu_S = \left(\frac{\partial T}{\partial p}\right)_S = \frac{T}{c_p}\left(\frac{\partial v}{\partial T}\right)_p. \tag{5.35}$$

Here the derivative in the second form corresponds to the volumetric coefficient of thermal expansion β, which is always positive for gases, which in turn means, that an isentropic expansion will always result in an temperature decrease, whereas the isentropic expansion only led to a decrease in certain cases. Furthermore an isentropic expansion over the same pressure range will always result in lower temperatures than an isenthalpic expansion. Additionally work can be recovered. The reason that isentropic valves are most commonly used in liquefaction systems, is that those work producing machines cannot handle significant phase changes, which is after all the desired result of liquefaction.

Traditionally only the isenthalpic expansion had been used within the cryogenic air separation process, since – as mentioned before – the air needs to be liquefied in order to be fed into be distilled. However in modern process configurations the isentropic expansion is also considered, and partial streams are fed into the low pressure column in gaseous form.

5.3 Heat exchange

The issue of heat integration is essential to the economic performance of cryogenic air separation. Foremost one must consider the special column configuration used in the process. Since operation of the condenser in the low pressure section only becomes possible if the reboiler in the high pressure section functions as heat sink, no external utilities are supplied to either unit. Rather they are

combined into a single heat exchange unit. Thus the absolute value of the reboiler energy must matched by the energy recovered from the condenser. Furthermore the material streams entering the process can – and should – exchange heat with the process streams leaving it. The combined condenser / reboiler for LPC / HPC column is assumed as a given heat exchange. This makes sense insofar, as this is a necessity in terms of the actual physical implementation of the process units. Also the usage of the oxygen rich liquid from the HPC as coolant in the Argon condenser is assumed as fixed.

This leaves the process stream leaving the compression stage of the process as well as all product and waste streams leaving the process. All those streams are – for simulation purposes and also in some process implementations – fed into a single multi-stream heat exchange unit. In actual processes all heat exchange and much of the process operations take place in the so called "cold box". As such a heavily insulated area is referred to. This is done to minimize heat exchange with the surroundings. Therefore and for further reasons compact heat exchange units such as plate-fin multi-stream heat exchangers are favoured when dealing with cryogenic processes in general and the cryogenic air septation in particular.

Due to the importance of heat integration to the ASU process some thought sould be given as to what modelling approach should be employed. Although the field of heat integration is one of the most intensively studied within process engineering, only a limited amount of approaches is available in open literature [17].

Traditionally heat integration has been carried out in a sequential manner, where it is for the purposes of process optimization assumed, that all heating and cooling is done by external utilities. After an (locally) optimal process configuration is identified, all hot and cold streams within the process are identified, and their temperature intervals fixed. In subsequent steps first the minimum utility requirements, and maximum number of heat exchangers are identified, and a specific heat exchange network (HEN) is designed. While this approach has been successfully applied to a multitude of processes and led to substantial savings, it is questionable if such a sequential approach will yield an optimal or near optimal solution.

Therefore some efforts have been made to develop efficient strategies for simultaneous process optimization and heat integration. Two general approaches can be distinguished. The first one based on the pinch concept. These methods are able to identify the minimum heat requirement as well as stream temperatures during process optimization. The first model along these lines was published by Duran and Grossmann [12] in 1986. They introduced a limited number of quite well behaved constraints into the optimization model to ensure no minimum driving force violations. Recently this model has been extended to handle phase changes and by fixing the utilities to zero been applied to the design of a multi-stream heat exchanger [17]. The major drawback with these methods is that one cannot target area of a given heat exchanger as the approach temperatures are not computed by the model. Therefore the sometimes substantial trade-off between the cost for heat exchange area and utility cost cannot be regarded.

A second approach employs superstructures of a HEN to find optimal matchings of process streams. No pinch point calculations are required, as the actual heat exchange is more or less modeled explicitly. This leads to the benefit, that approach temperatures as well as exchanged heat duties between each stream coupling are known within the model, and the cost of the designed unit can be considered in an economic objective function.
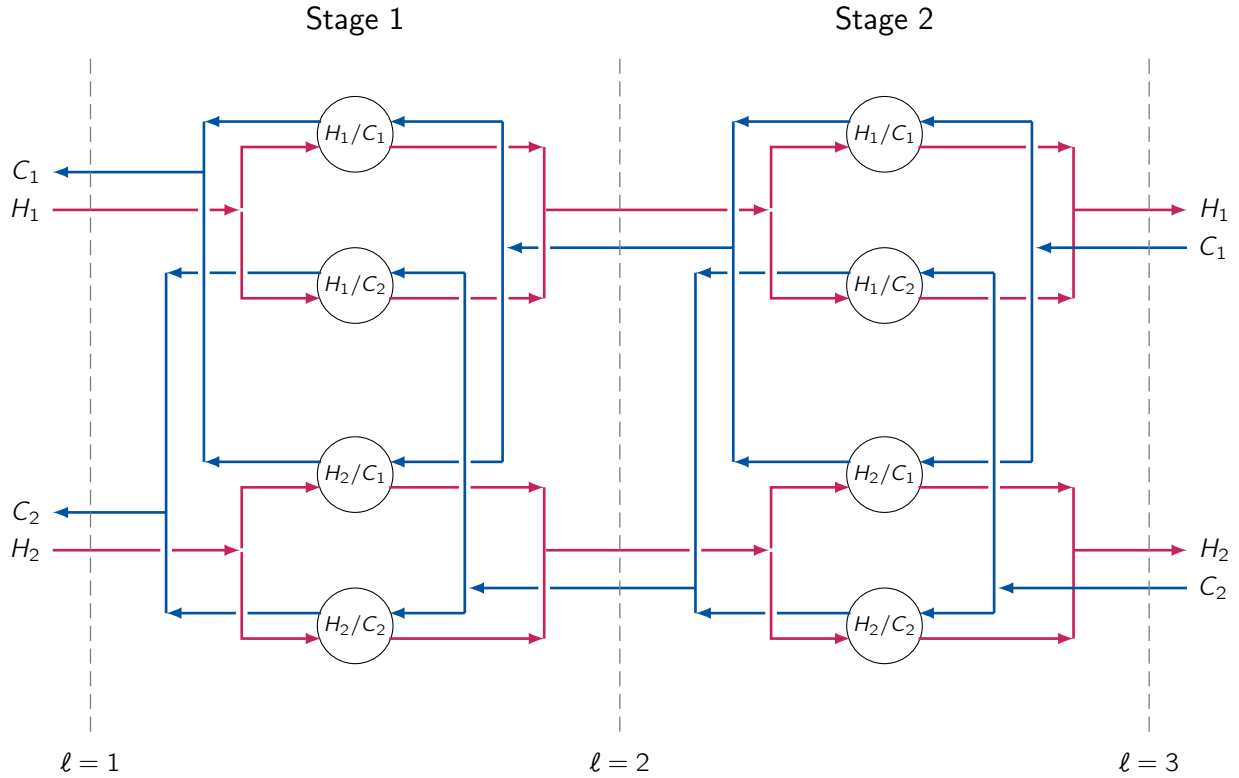
Figure 5.7: Superstructure for multi-stream heat exchanger. [25]

The approach and respective superstructure adapted in this thesis were first published by Yee and Grossmann [25]. Fig. 5.7 shows the stage wise superstructure for a HEN consisting of two hot and two cold streams.

In this stagewise structure each hot stream can exchange heat with each cold stream within each stage. The following assumptions were made when the model was developed

- Constant heat capacities

- Constant heat transfer coefficients

- Countercurrent heat exchangers

- Isothermal mixing at each stage.

The assumption of constant heat capacities is a common one in the design of HEN's. When no phase boundaries are passed and the temperature range of the involved is not too wide, it is a reasonably good approximation of the real conditions. While constant heat transfer coefficients a re assumed the model leaves the flexibility to define different coefficients for each pairing of hot and cold streams. Countercurrent heat exchangers are common in industrial practice. This assumption however does not really pose a limitation, as the model can easily be altered to account for concurrent units.

The last assumption of isothermal mixing is a more major one. It has been introduced as it allows for significant simplifications and leads to a model, where all constraints are linear and all non-linearities are restricted to the objective function. While that is certainly not true for the entire process model, it should at least allow for some reductions in the model complexity. The assumption states, that

regardless of which streams a given stream exchanges heat with, it will leave at the same temperature. Due to that all energy balances around each unit in the superstructure can be eliminated as well as the subsequent mixing of the streams.

Model equations First of all a heat balance at each stage is necessary

$$F_i(T_{i,\ell} - T_{i,\ell+1}) = \sum_j q_{ijk} \tag{5.36}$$

$$f_j(T_{i,\ell} - T_{i,\ell+1}) = \sum_i q_{ijk} \tag{5.37}$$

The heat exchange area A_{hx} can be computed from the exchanged energy, the heat transfer coefficients α_{ij} and the logarithmic mean temperature difference $LMTD$.

$$A_{hx} = \sum_i \sum_j \sum_k \frac{q_{ijk}}{\alpha_{ij} * LMDT_{ijk} + \delta} \tag{5.38}$$

While the small number δ is included to avoid problems in the program, when $LMDT$ becomes zero In order to avoid further numerical difficulties when the approach temperatures ΔT_{ij} at each side of an exchange unit approach zero, it was proposed to use an approximation introduced by Chen [10]

$$LMDT_{ijk} \approx \left[\Delta T_{ijk} \cdot \Delta T_{ijk+1} \frac{\Delta T_{ijk} + \Delta T_{ijk+1}}{2} \right]^{\frac{1}{3}} . \tag{5.39}$$

While the approach temperatures are defined as

$$\Delta T_{ijk} = \max\{0, T_{ik} - T_{jk}\} \tag{5.40}$$

AS the max function is non-smooth and thus non differentiable at the points $T_{ik} = T_{jk}$, gPROMS® internally uses a smooth approximation. The exact for of which is unknown to the author.

5.4 Thermodynamic models

Aside from the unit operation models, the behaviour of materials in a process needs to be adequately accounted for. This is done by means of so called equations of state (EOS) and excess Gibbs energy models. In terms of thermodynamics there are only a limited amount of variables. Namely the pressure, density and temperature as well as composition. While equations of state can model a given system in the vapour as well as liquid phase, excess Gibbs energy models only account for the behaviour of a liquid and need to be used in conjunction with other models for the vapour phase. However they have shown considerable better performance for highly non-ideal systems [3]. As mentioned earlier (sec. 5.2) it is essential to accurately capture the non-idealities of air in order to capture the liquefaction process. In the case of cryogenic air separation, the Peng-Robinson as well

as the Benders equation of state have shown satisfactory performance. The Peng-Robinson equation was chosen to be used in the presented model

$$p = \frac{RT}{V - b} - \frac{a_c \left[1 + m \left(1 - \sqrt{T_r}\right)\right]^2}{V^2 + 2bV - b^2} \tag{5.41}$$

$$m = 0.37464 + 1.54226\omega - 0.26992\omega^2 \tag{5.42}$$

$$a_c = 0.45724\frac{R^2 T_c^2}{p_c} \tag{5.43}$$

$$b = 0.077796\frac{RT_c}{p_c} \tag{5.44}$$

$$\omega = -1 - \log_{10}\left(p_r^{sat}\right)_{T_r = 0.7} \tag{5.45}$$

However the Peng-Robinson EOS relies on the so called one-fluid theory which models each fluid as pure. To model mixtures the pure component parameters have to be "mixed"

$$a = \sum_{i=1}^{C}\sum_{j=1}^{C} y_i y_j a_{ij}, \tag{5.46}$$

$$a_{ij} = \sqrt{a_i a_j}(1 - k_{ij}), \tag{5.47}$$

$$b = \sum_{i=1}^{C} y_i b_i. \tag{5.48}$$

From that EOS numerous relevant properties such as excess enthalpy, fugacity coefficients or densities can be calculated. For a list of some relevant equations refer to sec. A.1.

5.5 Economic models

As discussed earlier economic consideration play a major role in process design. In order to account for the process economics the cost of the process to be implemented needs to be estimated at the design level. However as limited information is available estimation methods have to be employed. In sec. 4 the general approach for cost estimation of process equipment was introduced, where a specific value such as heat-exchange area or vessel size is used to approximate equipment cost. However for more specific units extended models are available, where statistical data is employed to yield a more realistic fit to cost data. The cost functions and correction factors presented in this chapter are, if not stated otherwise, taken from [22]. Also unless otherwise stated the unit cost is given for the year 2006 ($CE = 500$).

Destillation column

Out of all the process equipment the distillation column probably is the most elaborate unit. It also poses the greatest challenges when it comes to finding an appropriate estimate for its cost. This is die to the fact that the column in itself is rather large and complex. To properly operate a column

the vessel needs to have numerous valves, scaffolding and several manholes. Due to its size further factors come into play that need not to be considered for the other relatively small units. Those location dependent factors might include resilience towards earthquakes, the ability to withstand close winds or intensive ambient temperatures. However as the scope of this work explicitly focuses on early design stages those location specific influences will be disregarded to arrive at simpler models for cost estimation.

Vertical tower   The cost for the vessel C_V which is to be vertically erected vertically is dependent on teh weight fo the weight W ($[lbs]$) of the vessel. This includes valves, manholes and other details directly connected with the tower. However the cost for ladders, platforms and railings necessary to properly operate the column are calculated separately

$$C_p = f_M\, C_V + C_{PL}. \tag{5.49}$$

The correlated equation for the cost of the tower is given by

$$C_V = \exp\left\{7.2756 + 0.18255 \cdot \ln[W] + 0.02297 \cdot (\ln[W])^2\right\}, \qquad 9000 \le W \le 2.5 \cdot 10^6. \tag{5.50}$$

To the cost of the tower, the cost of the surrounding support structure ist added. It is dependent on the inner diameter of the vessel (D_i) as well as the so called tangent to tangent length (L). This denotes the length of the tube that makes up the vessel excluding the spherical domes that close the column on each side. With that the additional cost is then computed by

$$C_{PL} = 300.9 \cdot (D_i)^{0.63316} \cdot (L)^{0.80161}. \tag{5.51}$$

Weight   As can be seen from the above correlations the weight of the column is a determining factor for the estimated and actual cost. Therefore some thought should be put into how this can be determined, when the final design is unknown. Again several correlations have been applied to real life units which yield satisfactory results. In general the weight of the empty vessel can be computed by determining the volume of the material and multiplying it with its density (ϱ)

$$W = \pi(D_i + t_s)(L + 0.8 \cdot D_i)t_s \cdot \varrho. \tag{5.52}$$

The term $0.8D_i$ is included to approximate the weight of the domes, whereas t_s is the shell thickness. To determine how thick the walls of the shell need to be the ASME pressure vessel code formula is often applied

$$t_s = \frac{P_d\, D_i}{2\, S\, E - 1.2 P_d}. \tag{5.53}$$

Where the maximal allowable stress S, which the chosen material can withstand at process conditions is multiplied by the fractional weld efficiency E to regard the effects of the manufacturing process on the material strength. To ensure an error on the side of caution the design pressure P_d is calculated from the actual operating pressure P_o by means of

$$P_d = \exp\left\{0.60600 + 0.91615 \cdot (\ln[P_o]) + 0.0015655 \cdot (\ln[P_o])^2\right\} \tag{5.54}$$

number of stages	shaft rpm	case-split orientation	flow rate range ([gpm])	pump head range ([ft])	maximum power ([Hp])	type factor f_T
1	3600	VSC	50 - 900	50 - 400	75	1.00
1	1800	VSC	50 - 3500	50 - 200	200	1.50
1	3600	HSC	100 - 1500	100 - 450	150	1.70
1	1800	HSC	250 - 5000	50 - 500	250	2.00
2	3600	HSC	50 - 1100	300 - 1100	250	2.70
2+	3600	HSC	100 - 1500	650 - 3200	1450	8.90

Table 5.3: Pump type factors [22].

It is important to consider, that the maximum allowable stress especially needs to take into account the operating temperature of the distillation process, as it might have significant effects.

Furthermore the given formulas only apply to pressures above ambient conditions. Thus low pressure or vacuum distillation is not covered by the presented formulas.

Column internals While internal support structures are already considered by the equations given above, the internals responsible to ensure product separation are not. Those make up a very significant amount of the total column cost and are available .

Centrifugal pump

Pumps are among the most common units of process equipment. While there are several different kinds of pumps that can be used, the centrifugal pump is one of the most popular choices and denotes a very likely choice for the process conditions considered in this application. Hence other pump types will not be considered at this point.

Pump In terms of operations pumps are best described by the volumetric flow transported Q as well as the pump head H, the hight that needs to be overcome. Data taken from the company Mosanto was used to correlate the pump cost to a specific value

$$S = Q\sqrt{H}. \tag{5.55}$$

As a reference unit the base price C_B is estimated for a cast iron single-stage vertically split case at 3600 *rpm*

$$C_B = \exp\left\{9.7171 - 0.6019 \cdot \ln[S] + 0.0519(\ln[S])^2\right\}, \qquad 400 \leq S \leq 100000. \tag{5.56}$$

The most influential addition factors for the pump price are the material, which is accounted for in the material factor f_m, as well as the rotation, case split orientation (horizontal and vertical), the number of stages, covered flow rate range, pump head range and maximum motor power, which are all agglomerated in the type factor f_T. Values for these factors are given in tab. 5.3 and tab. 5.4.

material of construction	material factor
cast iron	1.00
ductile iron	1.15
cast steel	1.35
bronze	1.90
stainless teel	2.00
Hastelloy C	2.95
monel	3.30
nickel	3.50
titanium	9.70

Table 5.4: Pump material factors [22].

type motor enclosure	3600 *rpm*	1800 *rpm*
open, drip-proof enclosure, 1 to 700 *Hp*	1.0	0.9
totally enclosed, fan-cooled, 1 to 250 *Hp*	1.4	1.3
explosion-proof encosure, 1 to 250 *Hp*	1.8	1.7

Table 5.5: Type factors for different motor types.

Electric motor   Separately from the pump itself the motor to drive the compression is considered. While the volumetric flow and the pump head certainly are valid choices to correlate motors for pumps especially, the power consumption is a more general specific value

$$P_C = \frac{P_T}{\eta_P \eta_M} = \frac{P_B}{\eta_M} \tag{5.57}$$

It can be calculated from the theoretic power of the pump P_T and the efficiencies η_P η_M. While an estimate for the expected power consumption might be already available at rather early design stages, the efficiencies will have to be correlated as well if resorting to average values is considered too coarse. Those correlations rely on the volumetric flow in gallons per minute ([gpm]) and the brake horse power $P_B = \frac{P_T}{\eta_P}$.

$$\eta_P = -0.316 + 0.24015 \cdot \ln[Q] - 0.01199 \cdot (\ln[Q])^2 \qquad 50 \leq Q \leq 5000 \tag{5.58}$$

$$\eta_M = 0.80 + 0.0319 \cdot \ln[P_B] - 0.00182 \cdot (\ln[P_B])^2 \qquad 1 \leq P_B \leq 1500 \tag{5.59}$$

After having calculated the power which the motor needs to supply its base cost of an open, drip-proof enclosed motor at 3600 *rpm* can be approximated by

$$C_B = \exp \left\{ 5.8259 + 0.13141 \cdot \ln[P_C] + 0.053255 \cdot (\ln[P_C])^2 \right.$$
$$\left. + 0.028628 \cdot (\ln[P_C])^3 - 0.0035549 \cdot (\ln[P_C])^4 \right\} \qquad 1 \leq P_C \leq 700 \tag{5.60}$$

To adjust the cost for different types of electric motors the type factors from tab. 5.5

Compressor

The cost of compressors is correlated with their respective power consumption measured in horsepower. Although not the most efficient type of compressor, centrifugal compressors are very popular in the process industry, as they are easily controlled an deliver a very steady flow. However as different types might be employed as well base cost correlations for centrifugal, reciprocation and screw compressors are given.

Centrifugal compressor

$$C_B = \exp\left\{7.5800 + 0.80 \cdot (\ln[P_C])\right\} \qquad 200 \le P_C \le 30000 \tag{5.61}$$

Reciprocating compressor

$$C_B = \exp\left\{7.9661 + 0.80 \cdot (\ln[P_C])\right\} \qquad 200 \le P_C \le 20000 \tag{5.62}$$

Screw compressor

$$C_B = \exp\left\{8.1238 + 0.7243 \cdot (\ln[P_C])\right\} \qquad 200 \le P_C \le 750 \tag{5.63}$$

Again as with most other equipment types correction factors are used to adjust for different realization of this piece of equipment. Here type of motor as well as the construction material have the biggest effects on the unit price and are explicitly considered.

$$C_p = f_D \, f_M \, C_B \tag{5.64}$$

The alternatives to the electric motor ($f_D = 1.0$) are a steam turbine ($f_D = 1.15$) or a gas turbine ($f_D = 1.25$). It should however be noted that aside from being the cheapest choice, the electric motor is also the most efficient. Thus the turbines are mostly considered, when process steam or combustion gas is easily available, such that the drawbacks might be eliminated by not having to supply the electric energy for the electric motor. In terms of construction material all base costs are for cast iron or carbon steel. Some appliances may require more resistant and also more expensive materials such as stainless steel ($f_M = 2.5$) or an nickel alloy ($f_M = 5.0$).

Reboiler / condenser

Reboiler and condenser can be characterized as heat exchangers, and be handled in the same way, as the main difference is weather heat is transferred to or from the process stream. In that sense they must be distinguished when considering the operating cost, as the cost for hot or cold auxiliary streams might differ significantly. As customary for heat exchangers the specific quantity for cost correlations is the necessary heat exchange area A measured in ft.

Again the construction material as well as the operating conditions have an effect on the final cost

$$C_p = f_P \, f_M \, C_B. \tag{5.65}$$

The correction for pressures f_P takes into account the operating pressure P_o and is computed by

$$f_P = 0.8510 + 0.1292 P_o + 0.0198 * P_o^2. \tag{5.66}$$

The material correction factor f_M

$$f_M = \tag{5.67}$$

Shell and tube heat exchanger

$$C_B = \exp\left\{ 11.667 - 0.8709 \cdot (\ln[A]) + 0.09005 \cdot (\ln[A])^2 \right\} \tag{5.68}$$

Double pipe

$$C_B = \exp\left\{ 7.146 + 0.1600 \cdot (\ln[A]) \right\} \tag{5.69}$$

5.6 Cryogenic air separation process

The roots of cryogenic air separation lie in the first experiment and apparatus by Carl von Linde – founder of the Linde AG – which led to the first air separation plant in 1902. This earliest version of the an air separation plant consisted of a single column or one might argue even only half a column as it only possess a reboiler and no condenser). In 1910 the foundation of to the modern air separation was set with the development of a double column plant. There each column operated at different pressures, which enabled the condenser and reboiler to be combined into a single heat exchange unit. This basic principle is in use to this day. However several enhancements have been made to to the original process design. Some were driven by new technological developments. Among the most prominent is the recovery of pure Argon – only a trace element in ambient air – within the process. Initially the Argon recovery had to be undertaken through the help of a catalytic converter. With the development of structured packings which display a very low pressure drop and height equivalent to theoretical stage (HEPT) it became feasible to separate Argon within a separate distillation column, as it requires a lot of theoretical stages, which would have previously led to infeasible large towers. Further advancements include internal compression which allows for compression of liquefied products within the cold box and more advanced designs of the condenser / reboiler unit.

For the purposes of this project a simplified version of an ASU has been considered. A process flowsheet is depicted in fig. 5.8.
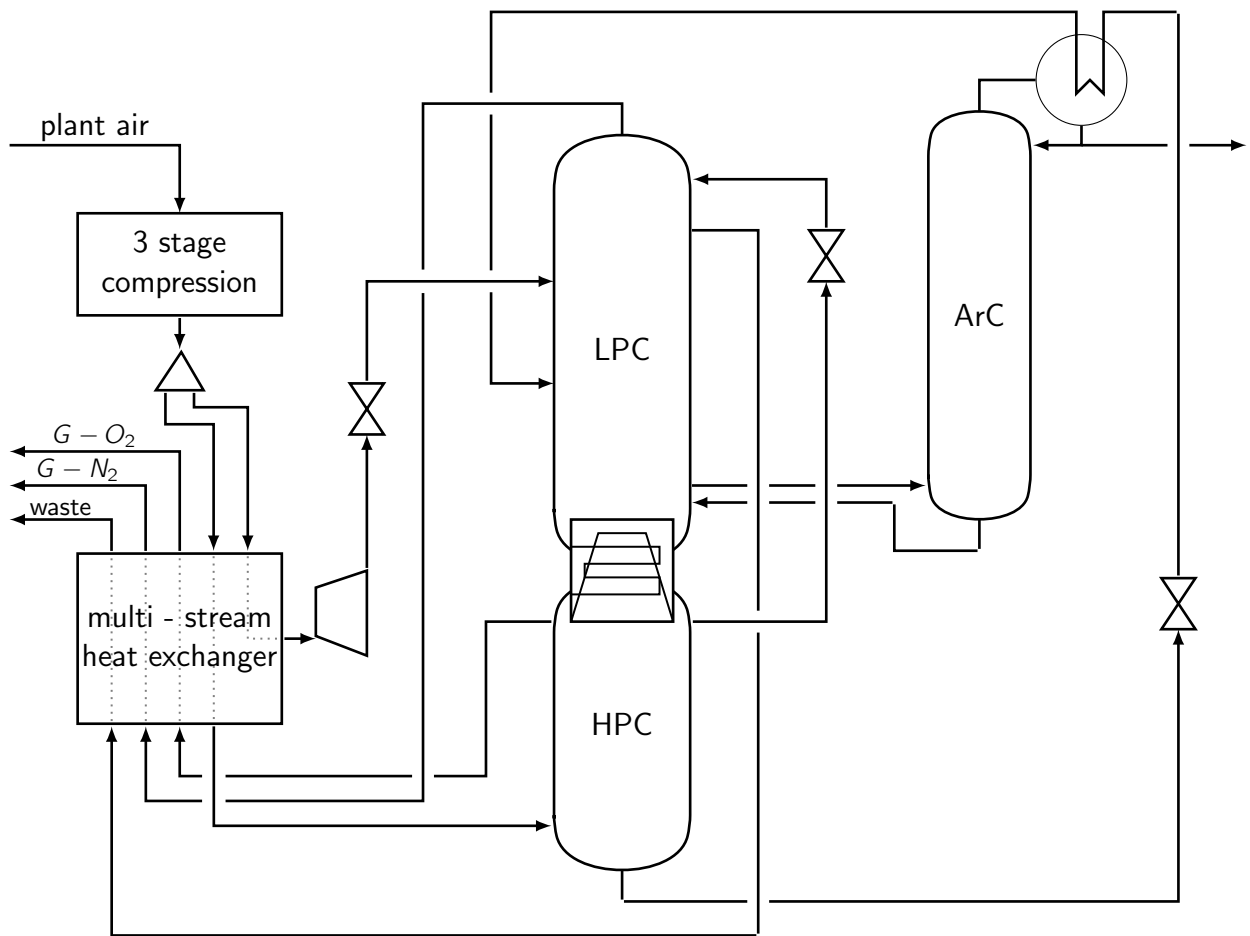
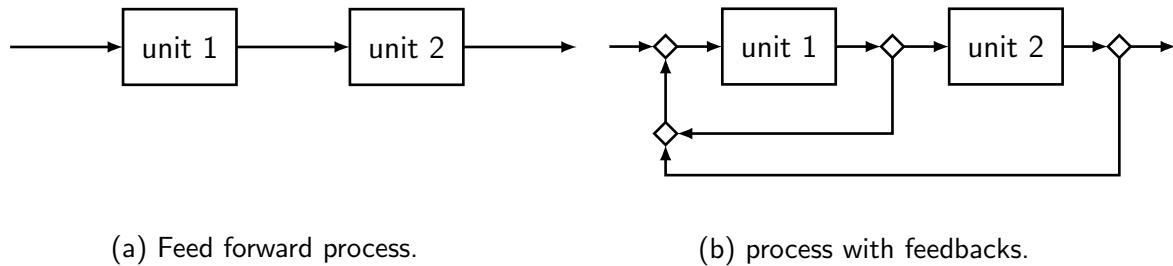Figure 5.8: simplified cryogenic air separation process.

(a) Feed forward process.   (b) process with feedbacks.

Figure 5.9: Different process configurations.

5.6.1 Flowsheet initialization

Even for single unit models initialization might pose difficulties, when a whole process model is considered, this task might become even more difficult. If the process units are mainly sequential, the task of initializing becomes no more difficult, then initializing the single units. But in most chemical processes a purely sequential arrangement of process equipment is not given. As soon as feedbacks are introduced into the process, the question of initialization becomes considerably more complex. In the most general case it is not even ensured, that a steady state of process operations even exists. As feedbacks are introduced, the process might become unstable or display oscillatory behaviour. Fig. 5.9a shows the concept for a purely feed forward process, while fig. 5.9b is an example for a process with feedbacks, in particular an arrangement with an inner and outer feedback loop.

As mentioned before feedbacks greatly complicate calculations for a given process. With the cryogenic air separation process this is especially true, since it is highly integrated and coupled. The only external cooling that is available comes from the initial compression and expansion of the ambient air. During the compression, since temperatures are still around ambient conditions and conventional coolants can be employed as heat sink. This is done during the multi-stage compression. All other heat exchange within the process can only be done against other internal process streams, as the process operates at conditions far away form ambient conditions. Far more than the feedbacks associated with material streams, it is the energy coupling that makes simulation of this process a non-trivial task. Especially, as the energies in condenser and reboiler of distillation columns have great effects on all operating condition.

Fig. 5.10 shows the flowsheet of the simplified ASU process depicted in fig. 5.8. In order the symbols in the material streams (blue) and energy streams (red) represend so called recycle breakers, which play a vital role during initialization of the flowsheet. The recycle breakers play no part in the converged flowsheet. Their function is to break the recycle or feedback loops in the process and transform the process into a feed forward process during initial computations. To achieve that, the recycle breakers are supplied with initial guesses for for all properties associated with the respective material or energy streams. For the energy recycle breakers the transformation from open to closed operation mode is rather simple. The outlet energy stream is merely moved from initial guess to inlet stream by means of eq. (5.32). For the material breaker one hast to invest a little more effort, as not all properties can be moved so easily while maintaining physical sense. The material stream and pressure are treated identically, while the temperature needs to computed from an enthalpy balance.

As for the concrete initialization procedure: first all recycle breakers are open and have the initial guesses at their outlet ports. Then all single units are converged. While this is done simultaneously
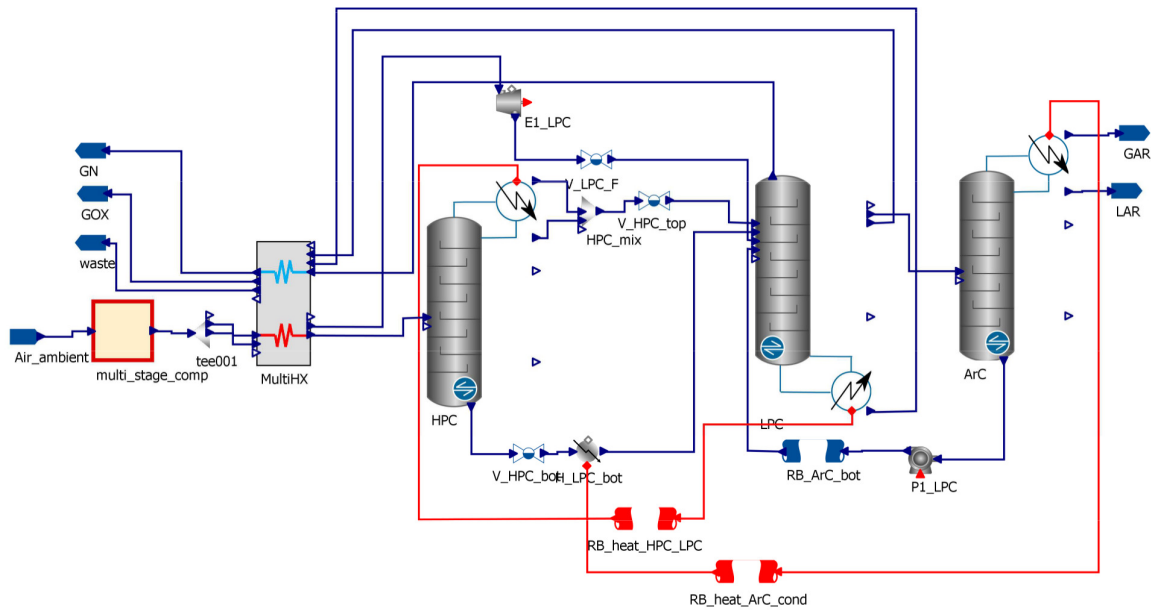
Figure 5.10: Implementation of simplified cryogenic air separation process in gPROMS.

in terms of the solution algorithm, the downstream units remain in the simplified stages of the unit respective initialization procedures wile the upstream units are solved with the rigorous models. Once all units have been converged, the recycle breakers are closed one after another. First the material stream between the Argon column (ArC) and the low pressure column (LPC), then the energy couple between the Argon condenser and and the oxygen rich material stream is closed. Finally the – maybe most important – connection between the LPC reboiler and HPC condenser is established.

6 Dynamic model

The previously described model is based on a steady state assumption. This means that all variables do not change with time. While a model like that offers valuable insight into the operation of a process many aspects remain unclear. In order to gain further insight into the process the dynamics have to be considered.

Due to that in this section a dynamic model of the ASU process will be developed.

6.0.2 column tray

balance equations

First the balance equations have to be rewritten in dynamic form. To do so reservoir terms or holdups are introduced. Namely the component holdups n_{ij} and internal energy U_j for each stage.
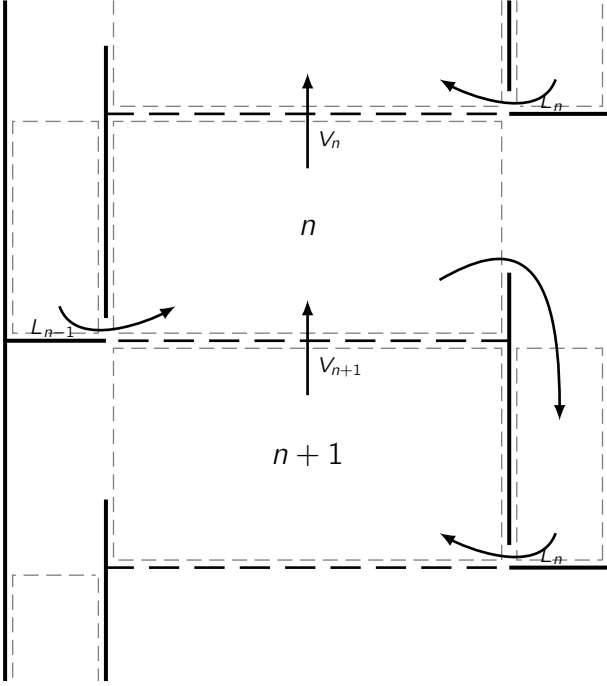
$n_C - 1$ **component balances**

$$\frac{\mathrm{d}n_{ij}}{\mathrm{d}t} = \left(1 + s_j^V\right) \cdot V_j \cdot y_{i,j} + \left(1 + s_j^L\right) \cdot L_j \cdot x_{i,j} - V_{j+1} \cdot y_{i,j+1}$$

$$- L_{j-1} \cdot x_{i,j-1} - \sum_{k=1}^{F^V} \zeta_{kj} \cdot F_j^V \cdot z_{i,j}^V - \sum_{l=1}^{F^L} \zeta_{lj} \cdot F_j^L \cdot z_{i,j}^L - \zeta_j^R \cdot V_N \cdot y_{iN},$$

$$i = 1 \dots n_C - 1, \quad j = 1 \dots N, \quad k = 1 \dots n_F, \quad l = 1 \dots n_F. \quad (6.1)$$

Total internal energy balance

$$\frac{\mathrm{d}U_j}{\mathrm{d}t} = \left(1 + s_j^V\right) \cdot V_j \cdot h_j^V + \left(1 + s_j^L\right) \cdot L_j \cdot h_j^L - V_{j+1} \cdot h_{j+1}^V$$

$$- L_{j-1} \cdot h_{j-1}^L - \sum_{k=1}^{F^V} \zeta_{kj} \cdot F_k^V \cdot h_j^{FV} - \sum_{l=1}^{F^L} \zeta_{lj} \cdot F_j^L \cdot h_j^{FL} - \zeta_j^R \cdot V_N \cdot h_N^V,$$

$$i = 1 \dots n_C, \quad j = 1 \dots n, \quad k = 1 \dots n_F, \quad l = 1 \dots n_F. \quad (6.2)$$

constituent equations

In addition to the balance equations further constituent equations need to be introduced. From the steady state model we know the equilibrium equations

$$y_{ij} = K_{ij} \cdot x_{ij}, \qquad i = 1 \ldots n_C \quad j = 1 \ldots N, \tag{6.3}$$

and the summation equations

$$1 = \sum_{i}^{n_c} y_{ij} \qquad j = 1 \ldots N, \tag{6.4}$$

$$1 = \sum_{i}^{n_c} x_{ij} \qquad j = 1 \ldots N. \tag{6.5}$$

Furthermore the mass accumulation in vapour n_j^V and liquid n_j^L phase as well as the energy accumulation need to be considered with

$$n_{ij} = x_{ij} n_j^L + y_{ij} n_j^V \qquad i = 1 \ldots n_C \quad j = 1 \ldots N, \tag{6.6}$$

$$U_j = n_j^L h_j^L + n_j^V h_j^V - p_j V_j \qquad j = 1 \ldots N. \tag{6.7}$$

$$\tag{6.8}$$

If pressure is to be computed within the model the tray volume constraint needs to be introduced

$$V_{tray} = \frac{n_j^V}{\varrho_j^V} + \frac{n_j^L}{\varrho_j^L} \qquad j = 1 \ldots N. \tag{6.9}$$

The liquid flow rates are determined by the hydraulic equations

$$h_j^{liq} - h^{weir} = 0.68175 F_w \left(\frac{q_j^L}{h_w} \right)^{\frac{2}{3}}. \tag{6.10}$$

$$\tag{6.11}$$

Where the height of the liquid on a stage is determined by the height of the liquid on a stage. It can be calculated form the liquid holdup on the respective stage

$$h_j^{liq} = \frac{n_j^L}{\varrho_j^L A_{active}} \qquad j = 1 \ldots N. \tag{6.12}$$

The pressure difference between stages is the driving force for the vapour streams. Teh pressure drop is modeled as having two contributions, the dray and wet pressure drop. While dry pressure drop stems from the vapour flowing through the holes with in tray, the wet pressure drop is caused by the liquid holdup on the stage.

$$p_j - p_{j+1} = h_j^{liq} \varrho_j^L g + 0.5 \xi \varrho_{j+1}^V \left(\frac{q_{j+1}^V}{A_h} \right)^2 \tag{6.13}$$

6.1 Models for columns with structured packings

- sections treated as trays
  - rate based models
    * film theory based models
  - equilibrium stage models
    * HETS / plate efficiency
- column divided into small (almost differential ?) sections
  - rate based models only

6.1.1 holdup & pressure drop

Model by Rocha et al.

equation for dimensionless holdup

$$h_t = \left(\frac{4 F_t}{S} \right)^{\frac{2}{3}} \sqrt[3]{\frac{3 \mu_L v_{LS}}{\varrho_L \sin(\theta) \varepsilon g_{eff}}} \tag{6.14}$$

correction factor for liquid holdup calculated ba Shi/Mersmann equation

$$F_{t,S-M} = \frac{29.12\,(We_L\,Fr_L)^{0.15}\,S^{0.359}}{Re_L^{0.2}\varepsilon^{0.6}(1 - 0.93\cos\gamma)(\sin\theta)^{0.3}} \tag{6.15}$$

$$g_{eff} = g\left(\frac{\varrho_L - \varrho_g}{\varrho_L}\right)\left[1 - \left(\frac{\Delta p/\Delta Z}{(\Delta p/\Delta Z)_{flood}}\right)\right] \tag{6.16}$$

$$\cos\gamma = \begin{cases} 0.9 & \text{if } \sigma \leq 0.055\frac{N}{m} \\ 5.211\cdot 10^{-16.835\sigma} & \text{if } \sigma > 0.055\frac{N}{m} \end{cases} \tag{6.17}$$

$$Re_L = \frac{\varrho_L v_L D}{\mu_L} \tag{6.18}$$

$$We_L = \frac{\varrho_L v_L^2 D}{\sigma} \tag{6.19}$$

$$Fr_L = \tag{6.20}$$

dry pressure drop with correlated friction factor funktion...

$$\frac{\Delta p_{dry}}{\Delta Z} = \underbrace{\frac{0.177\varrho_g}{S\varepsilon^2(\sin\theta)^2}}_{A}\cdot v_{gS}^2 + \underbrace{\frac{88.774\mu_g}{S^2\varrho\sin\theta}}_{B}\cdot v_{gS} = Av_{gS}^2 + Bv_{gS} \tag{6.21}$$

Delft model

- valid in pre-load region
- adjustment by loading factor (Olujic 1999)

SPR method

- valid in pre-load region
- adjustment by loading factor (Olujic 1999)

Hydrodynamic analogy

- employ rigorous methods to solve hydrodynamics by superimposing solutions of easier scenarios

gas flow

- assume round channels with hydraulic diameter
- laminar fully developed flow
- ideal mixing at regular intervals to account for abrupt changes in gas flow directions at intersections

liquid flow

- continous thin film flow
- flow direction according to gravity flow angle
- laminar fully developed flow
- neglect of radial maldistribution
- ideal mixing at periodic intervals

equations   hydraulic diameter

$$d_h = \frac{b_0 h}{s_0} \tag{6.22}$$

gravity flow angle

$$alpha = \arctan \left(\frac{\cot \varphi}{\sin \left[\arctan \left(\cos \varphi \cot \frac{\gamma}{2} \right) \right]} \right) \tag{6.23}$$

undisturbed liquid flow

$$z_L = \frac{b_0}{2 \sin \left(\frac{\gamma}{2} \right) \sin \beta} \tag{6.24}$$

$$\beta = \arcsin \left(\sin \varphi \cos \epsilon \right) \tag{6.25}$$

$$\epsilon = \arctan \left(\cos \varphi \cot \frac{\gamma}{2} \right) \tag{6.26}$$

undisturbed gas flow

$$\ell_i = \frac{2 B_i L}{b_0} \tag{6.27}$$

hydrodynamic equations

$$0 = \mu_p \left(\frac{\partial 2}{\partial u_p} y \right) - \frac{\partial P_p}{\partial x} + g \varrho_p \sin \alpha, \tag{6.28}$$

$$\frac{\partial P_p}{\partial y} = 0, \qquad p = L, G \tag{6.29}$$

$$\frac{\partial p_L}{\partial x} = \frac{\partial p_L}{\partial y} = const = \Delta p \tag{6.30}$$

$$u_L|_{y=0} = 0 \qquad u_L|_{y=\delta} = u_G \tag{6.31}$$

7 Conclusion and further research

Bibliography

[1] D. Acharya, F. Fitch, and R. Jain. Some Issues in Operating Adsorption Prepurification Systems for Cryogenic Air Separation. *Separation Science and Technology*, 31(16):2171–2182, 1996.

[2] Charles O. Akinlabi, Dimitrios I. Gerogiorgis, Michael C. Georgiadis, and Efstratios N. Pistiko-poulos. Modelling, Design and Optimisation of a Hybrid PSA-Membrane Gas Separation Process. In V. Plesu and P. S. Agachi, editors, *17TH EUROPEAN SYMPOSIUM ON COMPUTER AIDED PROCESS ENGINEERING*, volume 24 of *Computer-Aided Chemical Engineering*, pages 363–370, SARA BURGERHARTSTRAAT 25 and PO BOX 211 and 1000 AE AMSTERDAM and NETHERLANDS, 2007. ELSEVIER SCIENCE BV.

[3] Andreas Pfennig. *Thermodynamik der Gemische.* Springer-Verlag, 2003.

[4] Randall F. Barron. *Cryogenic systems.* Oxford University Press and Clarendon Press, New York and Oxford [Oxfordshire], 2 edition, 1985.

[5] Mariana Barttfeld and Pío A. Aguirre. Optimal Synthesis of Multicomponent Zeotropic Distilla-tion Processes. 1. Preprocessing Phase and Rigorous Optimization for a Single Unit. *Industrial & Engineering Chemistry Research*, 41(21):5298–5307, 2002.

[6] F. P. Bernardo, Efstratios N. Pistikopoulos, and Pedro M. Saraiva. Quality costs and robustness criteria in chemical process design optimization. *Computers & Chemical Engineering*, 25(1):27–40, 2001.

[7] J. F. Boston and S. L. Sullivan. A new class of solution methods for multicomponent, multistage separation processes. *The Canadian Journal of Chemical Engineering*, 52(1):52–63, 1974.

[8] BOSTON J. F. Inside-Out Algorithms for Multicomponent Separation Process Calculations: 7. In *Computer Applications to Chemical Engineering*, pages 135–151.

[9] W. F. Castle. Air separation and liquefaction: recent developments and prospects for the beginning of the new millennium. *International Journal of Refrigeration*, 25(1):158–172, 2002.

[10] J. J. J. Chen. Letter to the Editor: Comments on improvement on a replacement for the logarithmic mean. *Chemical Engineering Science*, 42:2488–2489, 1987.

[11] Guido Dünnebier and Constantinos C. Pantelides. Optimal Design of Thermally Coupled Distillation Columns. *Industrial & Engineering Chemistry Research*, 38(1):162–176, 1999.

[12] M. A. Duran and Ignacio E. Grossmann. Simultaneous optimization and heat integration of chemical processes. *AIChE Journal*, 32(1):123–138, 1986.

[13] Roger Fletcher and William Morton. Initialising distillation column models. *Computers & Chemical Engineering*, 23(11-12):1811–1824, 2000.

[14] Ignacio E. Grossmann, Pío A. Aguirre, and Mariana Barttfeld. Optimal synthesis of complex distillation columns using rigorous models. *Computers & Chemical Engineering*, 29(6):1203–1215, 2005.

[15] K. P. Halemane and Ignacio E. Grossmann. Optimal process design under uncertainty. *AIChE Journal*, 29(3):425–433, 1983.

[16] Ernest J. Henley, J. D. Seader, and D. Keith Roper. *Separation process principles*. John Wiley & Sons, Chichester, 3 edition, op. 2011.

[17] Ravindra S. Kamath, Lorenz T. Biegler, and Ignacio E. Grossmann. Modeling multistream heat exchangers with and without phase changes for simultaneous optimization and heat integration. *AIChE Journal*, 58(1):190–204, 2012.

[18] P. Mahapatra and B. W. Bequette. Process design and control studies of an elevated-pressure air separations unit for IGCC power plants: American Control Conference (ACC), 2010: American Control Conference (ACC), 2010 DOI -. *American Control Conference (ACC), 2010*, pages 2003–2008, 2010.

[19] Leonard M. Naphtali and Donald P. Sandholm. Multicomponent separation calculations by linearization. *AIChE Journal*, 17(1):148–153, 1971.

[20] Max Stone Peters, Klaus D. Timmerhaus, and Ronald E. West. *Plant design and economics for chemical engineers*. McGraw-Hill, New York, 5 edition, 2003.

[21] R. Prasad, F. Notaro, and D.R Thompson. Evolution of membranes in commercial air separation. *Journal of Membrane Science*, 94(1):225–248, 1994.

[22] W. D. Seider, J. D. Seader, D. R. Lewin, and S. Widagdo. *Product and Process Design Principles: Synthesis, Analysis, and Evaluation*. J. Wiley, New York, 3 edition, 2010.

[23] Avinash R. Sirdeshpande, Marianthi G. Ierapetritou, Mark J. Andrecovich, and Joseph P. Naumovitz. Process synthesis optimization and flexibility evaluation of air separation cycles. *AIChE Journal*, 51(4):1190–1200, 2005.

[24] Phillip C. Wankat and Kyle P. Kostroski. Hybrid Membrane-Cryogenic Distillation Air Separation Process for Oxygen Production. *Separation Science and Technology*, 46(10):1539–1545, 2011.

[25] T.F Yee, Ignacio E. Grossmann, and Z. Kravanja. Simultaneous optimization models for heat integration—I. Area and energy targeting and modeling of multi-stream exchangers. *Computers & Chemical Engineering*, 14(10):1151–1164, 1990.

[26] Yu Zhu, Sean Legg, and Carl D. Laird. Optimal design of cryogenic air separation columns under uncertainty: Selected papers from the 7th International Conference on the Foundations of Computer-Aided Process Design (FOCAPD, 2009, Breckenridge, Colorado, USA. *Computers & Chemical Engineering*, 34(9):1377–1384, 2010.

A Appendix A

A.1 Peng-Robinson derived properties

The Peng-Robinson equation of state cab be rewritten as a cubic polynomial in terms of the compressibility factor $Z = \frac{pv}{RT}$

$$0 = Z^3 + \alpha Z^2 + \beta Z + \gamma \tag{A.1}$$

$$\alpha = B - 1 \tag{A.2}$$

$$\beta = A - 2B - 3B^3 \tag{A.3}$$

$$\gamma = B^3 + B^3 - AB \tag{A.4}$$

$$A = \frac{ap}{(RT)^2} \tag{A.5}$$

$$B = \frac{bp}{RT} \tag{A.6}$$

The *Joule-Thompson* factor cab be expressed as

$$\mu_{JT} = \frac{1}{c_p} \left[T \left(\frac{\partial v}{\partial T} \right)_p - v \right] \tag{A.7}$$

and in terms of the compressibility factor

$$\left(\frac{\partial v}{\partial T} \right)_p = \frac{R}{p} \left[T \left(\frac{\partial Z}{\partial T} \right)_p + Z \right] \tag{A.8}$$

$$\left(\frac{\partial Z}{\partial T} \right)_p = \frac{\left(\frac{\partial A}{\partial T} \right)_p (B - Z) + \left(\frac{\partial B}{\partial T} \right)_p (6BZ + 2Z - 3B^2 - 2B + A - Z^2)}{3Z^2 + 2(B - 1)Z + (A - 2B - 3B^2)} \tag{A.9}$$

$$\left(\frac{\partial A}{\partial T} \right)_p = \frac{p}{(RT)^2} \left(a' - \frac{2a}{T} \right) \tag{A.10}$$

$$\left(\frac{\partial B}{\partial T} \right)_p = \frac{-bp}{RT^2} \tag{A.11}$$

$$a' = \frac{da}{dT} = \frac{1}{2} \sum_{i=1}^{C} \sum_{j=1}^{C} w_i w_j (1 - k_{ij}) \left(\sqrt{\frac{a_j}{a_i}} a_i' + \sqrt{\frac{a_i}{a_j}} a_j' \right) \tag{A.12}$$

$$a_i' = \frac{da_i}{dT} = \frac{-m_i a_i}{\left[1 + m_i (1 - \sqrt{\frac{T}{T_{ci}}}) \right] \sqrt{T T_{ci}}} \tag{A.13}$$

$$\ln \varphi = \frac{1}{RT} \int_0^p \left(V - \frac{RT}{p} \right) dp, \tag{A.14}$$

$$\ln \varphi = (Z - 1) - \ln Z - \int_\infty^V \frac{Z - 1}{V} dV \tag{A.15}$$

$$\ln \varphi_i = \frac{b_i}{b}(Z - 1) - \ln \left[Z \cdot \left(1 - \frac{b}{V} \right) \right]$$
$$+ \frac{1}{bRT} \left[\frac{\sqrt{2}ab_i}{4b} - \sqrt{\frac{aa_i}{2}} \right] \ln \left(1 + \frac{b}{V} \right) \left(\frac{1 + \frac{b}{V} \left(1 + \sqrt{2} \right)}{1 + \frac{b}{V} \left(1 - \sqrt{2} \right)} \right) \tag{A.16}$$